PROTECTION FROM SCOUR OF BRIDGE PIERS USING RIPRAP

Transfund New Zealand Research Report No. 82

PROTECTION FROM SCOUR OF BRIDGE PIERS USING RIPRAP

R.N. CROAD
Opus International Consultants Ltd
Central Laboratories, Lower Hutt

Transfund New Zealand Research Report No. 82

ISBN 0-478-10540-1
ISSN 1174-0574

PO Box 2331, Lambton Quay, Wellington, New Zealand
Telephone (04) 473-0220; Facsimile (04) 499-0733

Croad, R.C. 1997. Protection from scour of bridge piers using riprap. *Transfund New Zealand Research Report No. 82.* 53 pp.

Keywords: bridges, bridge scour, hydraulic design, scour protection, riprap, roads

AN IMPORTANT NOTE FOR THE READER

The research detailed in this report was commissioned by Transit New Zealand when it had responsibility for funding roading in New Zealand. This funding is now the responsibility of Transfund New Zealand.

While this report is believed to be correct at the time of publication, Transit New Zealand, Transfund New Zealand, and their employees and agents involved in preparation and publication, cannot accept any contractual, tortious or other liability for its content or for any consequences arising from its use and make no warranties or representations of any kind whatsoever in relation to any of its contents.

The report is only made available on the basis that all users of it, whether direct or indirect, must take appropriate legal or other expert advice in relation to their own circumstances and must rely solely on their own judgement and seek their own legal or other expert advice.

The material contained in this report is the output of research and should not be construed in any way as policy adopted by Transit New Zealand or Transfund New Zealand but may form the basis of future policy.

ACKNOWLEDGMENTS

The contributions of the following persons during the course of this research programme are gratefully acknowledged:

Messrs E. Kerschbaumer, J.G.A. Arts, W.E. Hickman, Ms S. Page and Dr F.D. Edmonds of Central Laboratories, Opus International Consultants Ltd, Lower Hutt.

Mr J.F. McGuire of Transit New Zealand, Wellington.

CONTENTS

EXECUTIVE SUMMARY

1. Introduction

The results of an experimental study carried out in 1993 of the use of riprap to protect bridge piers against scour are summarised. Experiments involved two sizes of bed sediment and two sizes of riprap. Four pier shapes were used in the experiment: circular, square and two slab shapes, representative of bridge designs built before 1960.

2. Experimental Studies

A total of 32 experiments were completed. The first set of 16 experiments was carried out in a 0.45 m wide tilting flume in which each pier was considered in isolation. The second set of experiments was carried out in a 1.5 m wide flume in which the interactions between adjacent piers and between a pier and an adjacent abutment were considered. All experiments involved general sediment transport and bed lowering with shear stresses reaching up to two times the value required to initiate sediment transport.

The present study is a continuation of an earlier (1990) preliminary experimental study of bridge pier scour protection using riprap in which the flow approaching the piers was just below the condition of flow required to initiate sediment transport (clear water scour conditions). The report also reviews other literature on riprap protection of bridge piers.

3. Theory

A theory for the design of stable riprap mats around bridge piers is developed. The theory considers three important aspects: the stability of the riprap against entrainment into the flow; the ability of the riprap to embed into the underlying sediment; and the compatibility of the filter layer with riprap and of riprap with the bed sediment. The theory is compared with experimental data from this report and other published sources.

4. Design Procedure

A procedure for the design of bridge pier riprap protection systems is presented in an Appendix. The procedure incorporates the findings of the study, and specifies how to determine the required riprap stone size, and the plan and elevation dimensions required for the riprap mat. A worked example for a circular pier demonstrates the application of the procedure.

Because the riprap is generally required to protect the pier against relatively low probability events, and since the proposed riprap size design equation forms a lower bound to the data, a low factor of safety (F) of 1.25 is recommended for design.

The following additional features or constraints are recommended:

- The riprap layer should be placed below the trough of any dunes that may exist in the river during floods.

- The spacing between the piers has not been tested as a variable. The results are based on a pier spacing in the order of 16 m measured centre to centre and at skew angles up to 30°, which is reasonably representative of slab bridges built in the 1940-70 era. For very short spacings (say less than 13 m) and very high skew angles (greater than 30°), specific model tests will be warranted.

- For piers with abutments, the design should be based on a velocity taken at a midpoint between the abutment and the pier (rather than on the upstream approach velocity which will be lower). For very complicated geometries or very high skew angles, a physical model will be warranted in which case the riprap can be tested directly.

ABSTRACT

The results of an experimental study carried out in 1993 of the use of riprap to protect bridge piers against scour are presented. Experiments involved several sizes of bed sediment and riprap, and different types of bridge piers, under conditions involving general sediment transport and bed lowering. The interaction between adjacent piers and between a pier and an adjacent abutment is considered.

A theoretical basis for the design of the riprap, considering stability against entrainment into the flow, embedment into the underlying sediment, and compatibility of filter layer with riprap layer, and of riprap with bed sediment is developed. A complete design procedure, and an example, for the design of riprap pier scour protection systems is appended.

1. INTRODUCTION

1.1 Background

In a survey of 108 failures of bridges, occurring on the New Zealand road network during the period 1960 to 1980, 70 failures could be attributed to scour, and of these 34 were the result of local scour at piers (Sutherland 1986). The pier failures typically related to bridges built before 1960 (although there were a few exceptions) which had been built with relatively shallow foundations of 6 to 8 metres depth.

The placing of riprap mats around bridge piers seems to be an attractive method of protecting bridge piers against scour. Breusers et al. (1977) suggest that the placement of riprap mats is the only type of protection system that totally prevents scour. Nonetheless, the practice of using riprap protection around bridge piers is uncommon in New Zealand. In examples where riprap mats have been applied, experiences of their effectiveness have been conflicting.

Riprap mat systems used on the piers of the Wairoa bridge (State Highway SH2, Gisborne) and the Awatere bridge (SH35, Marlborough) have failed or been ineffective. A mat, 1.0 m thick placed across the full width of the river using 0.35 m minimum-diameter rock, has been successful at Ruamahanga bridge (SH2 at Te Ore Ore, Wairarapa), although maintenance repairs have been required. Scour protection planned at the Waingawa bridge (SH2, Wairarapa) was not implemented. One of the Waingawa bridge piers subsequently failed due to scour. As part of the remedial work, riprap was again considered but, without a reliable design method, the conservative design estimate of the stone size required was found to be too large and a foundation underpinning option was finally adopted.

A preliminary study of riprap protection at bridge piers was carried out before 1990 at Opus International Consultants Ltd Central Laboratories (Opus), Lower Hutt, involving clear water scour conditions (Croad 1990). Tentative formulae for predicting the required riprap size were given. It was found that riprap can be effective in controlling pier scour provided that special conditions are met (discussed in Section 1.2 of this report).

In order to develop a reliable method for the design of riprap mats, experiments involving general sediment transport need to be carried out, using three-dimensional flow conditions. Those conditions are the purpose of the experimental work carried out at Opus in 1993 and reported here.

Figure 1.1 Report by Engels (1929) on experiments on the use of riprap to protect a bridge pier against scour (in Posey 1974).

A. EXPERIMENTS PERTAINING TO THE PROTECTION OF BRIDGE PIERS AGAINST UNDERMINING [1]

When these experiments were undertaken, in 1893, it was the general opinion that the danger to pier foundations occurred particularly at the downstream end of the piers. The experiments performed on small models showed the contrary, viz., that the scouring action occurred at the upper end and caused the pier to tip upstream when the foundations of the models were not set deep enough in the sand layer. The studies that have now been made on actual bridge catastrophes caused by high water have proved the results obtained with these models. Further experiments that were made with the models, covering the proper measures to be taken for the protection of pier foundations, gave valuable results for practice. These experiments demonstrated that the method formerly employed of encircling the pier with stone riprap up to the low-water mark should be discarded, and that it was of far greater importance to excavate the material around the upstream end of the pier and fill in with riprap flush with the bed of the stream (Figs. 52 and 53). And what is the scientific significance of these experiments? An expenditure of approximately 300 marks ($75) to obtain knowledge that resulted in the yearly saving of thousands of dollars. With reference to sums expended for stone riprap we refer to one example only, viz., the "protection," in accordance with the old faulty method, of the piers of the Weichsel Bridge at Fordon. The cost of stone riprap alone for each pier amounted to 46,000 marks ($11,000), and in addition thereto there was a yearly maintenance cost of 400 marks ($100).

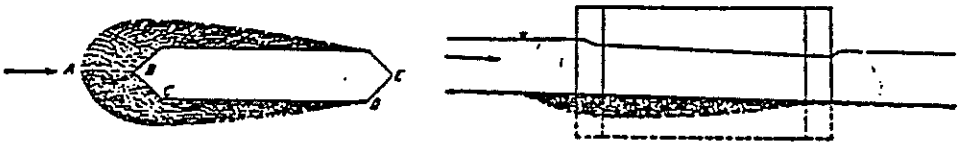

FIGS. 52 and 53 Protection of a River Pier—Plan and Longitudinal Section

Figure 1.2 Riprap mat plan dimensions for bridge piers recommended by Gales (1938).

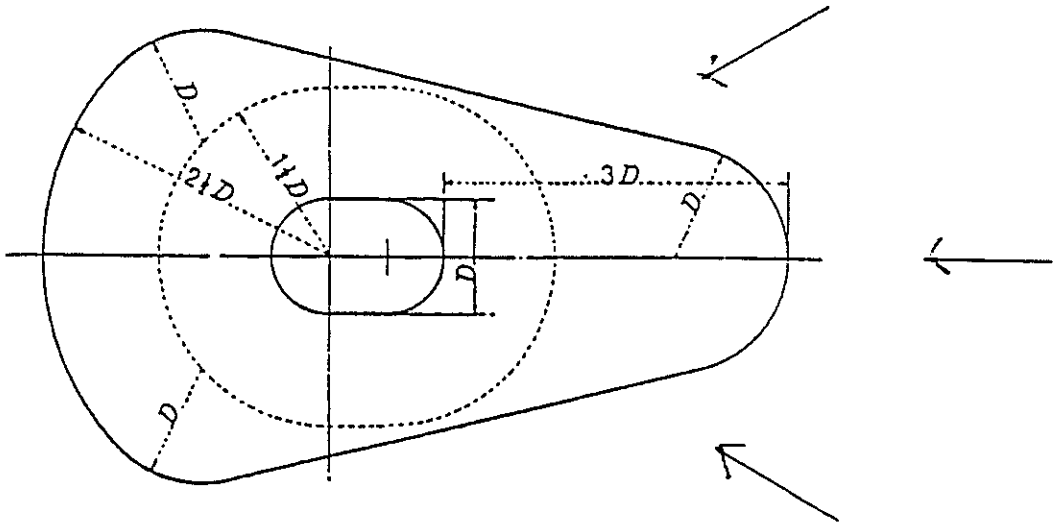

1.2 Previous Research

A very early report of the use of riprap to prevent scour around a bridge pier, based on the results of hydraulic model experiments undertaken in 1893, was given by Engels (1929) (also reproduced in Posey 1974). The relevant text is here reproduced from the original as Figure 1.1.

Another early report of the use of riprap mats to protect bridge piers against scour was given by Gales (1938) who recommended that the riprap be placed around the pier in a pear shape, as shown in Figure 1.2. A mat thickness of 1.5 times the riprap stone size was suggested. The size of riprap was linked to the class of the river, being either A, B or C dependent on the discharge as defined in Gales (1938). Gales applied these designs to bridges in India that had shallow foot foundations. The riprap mats were intended to prevent scour around the edges of the slab foundation. Nevertheless, Gales had to report ... *In all cases in active rivers the expenditure on replacing the stone around the piers has been enormous, partly owing to some misunderstanding of the purpose of the pitching, and partly to the difficulty experienced in verifying the position of the stone after the subsidence of floods. ...*

The plan dimensions for riprap mats given by Gales (1938) were also recommended by Farraday and Charlton (1983). These authors also suggested applying the formula used by Maynord (1978) to determine the riprap size, namely

$$\frac{D_{50}}{h} = C\frac{U_{max}^3}{(gh)^{3/2}} \qquad (1)$$

in which D_{50} is the median stone size of the riprap, h is the water depth, U_{max} is the maximum design velocity, g is the gravitational acceleration, and C is a coefficient in the range 0.22 to 0.28 corresponding to factors of safety of 1.0 to 2.0 respectively.

In Equation 1, factor of safety is the ratio of riprap mass to the mass for incipient motion conditions for a given velocity U_{max}. The maximum velocity is related to the upstream approach velocity by a multiplier as given in Table 1.1.

Table 1.1 Multipliers to relate maximum flow velocity with upstream approach velocity (after Farraday and Charlton 1983).

Location	Multiplier
At noses of groynes and guide banks	2.0
At bends	1.5
In straight reaches	1.25

It is implied from an example given by Farraday and Charlton (1983) that a multiplier of 1.25 should be applied to the design of riprap around bridge piers.

Farraday and Charlton also gave guidelines on the grading of the riprap, based on the recommendations of Simons and Senturk (1977) who stated that the ratio of the maximum riprap size to median D_{50} size should be about 2.0, and the ratio between the D_{50} and D_{20} sizes should also be about 2.0. A filter layer beneath the riprap was also recommended based on the following specification:

$$\frac{d_{50}\ (\text{layer}\ 1)}{d_{50}\ (\text{layer}\ 2)} < 40$$

$$5 < \frac{d_{15}\ (\text{layer}\ 1)}{d_{15}\ (\text{layer}\ 2)} < 40 \qquad (2)$$

$$\frac{d_{15}\ (\text{layer}\ 1)}{d_{85}\ (\text{layer}\ 2)} < 5$$

in which "d" is a sediment size of the layer 1 or layer 2 as indicated. The specification given by Equation 2 applies simultaneously between the riprap (layer 1) to the filter layer (layer 2), as well as the filter layer (layer 1) and the underlying bed sediment (layer 2).

Breusers et al. (1977) suggested the formula:

$$U_0 = 0.42\ \sqrt{2\Delta g D_{50}} \qquad (3)$$

for the design of the riprap size around bridge piers in which U_0 is the maximum approach velocity, and Δ is the submerged relative density of the riprap. Equation 3 is based on a formula from Isbash (1935) for determining the critical stable size of rock under flowing water, after assuming the local velocity around the pier to be twice that of the approach flow according to Carstens (1966). Hancu (1971) and Ramette and Nicollet (1971) also showed that scour commences around circular piers at an approach velocity equal to half the incipient motion velocity for the bed material.

Breusers et al. (1977) also recommended that a filter layer is required below the riprap layer on the basis of tests carried out by Posey (1974) who used the Terzaghi-Vicksburg specification:

$$\frac{d_{50}\ (\text{filter})}{d_{50}\ (\text{base})} < 25$$

$$4 < \frac{d_{15}\ (\text{filter})}{d_{15}\ (\text{base})} < 20 \qquad (4)$$

$$\frac{d_{15}\ (\text{filter})}{d_{85}\ (\text{base})} < 5$$

Posey (1974) recommended that the pier protection should extend a distance of 1.5 to 2.5 pier diameters in all directions from the face of the pier. The emphasis in Posey's study was on treating the riprap mat as a filter and no definite guidelines were given on how to determine the stable size.

Posey stated that ... *For the design of permanent new bridges, sole dependence upon the method described in these model tests is not recommended. It can be used where minor settlement or enough undermining has occurred to cause apprehension over safety. The results of such installations should be reported to the profession.* ...

Hjorth (1975) theoretically and experimentally studied the flow field around circular and square piers to determine the distribution of velocity, shear stress, and zone disturbed by the pier. Hjorth found that a bed area equal to B on either side, ½B on the upstream side and 3B on the downstream side was affected by the accelerated flow around the pier, in which B is the width of the pier. The affected zone formed a tear drop shape. Hjorth's experimental measurements also provided some data on the incipient erosion velocity for two sediment sizes around the piers which are summarised in Table 1.2.

Table 1.2 Summary of data recorded by Hjorth (1975).

Shape of Pier	U_0 (m/s)	D (mm)	h (m)	Comment
circular	0.35	2 to 4	0.25	eroded
circular	0.35	4 to 8	0.25	stable
square	0.35	2 to 4	0.25	eroded
square	0.35	4 to 8	0.25	stable

U_0 = average approach velocity; D = riprap size; h = depth of water

Croad (1990) carried out an experimental study of riprap protection around bridge piers under clear water scour conditions. Croad suggested that the riprap be placed flush with the bed level and that the riprap layer be at least two stone diameters thick. He also found, as have others, that the compatibility of the riprap size with the bed material size must be considered, but also that special attention must be paid to the placement of riprap around the pier. The ravelling loss of riprap from the downstream edge of the riprap mat was an important cause of riprap failure.

The data from this study are summarised in Table 1.3 in which d_{50} is the median bed material size, D_{50} is the median riprap size, d_s is the depth of scour measured below the bed level, and other symbols are as already defined.

Croad (1990) proposed the expression:

$$\frac{U_{max}}{\sqrt{\Delta g D_{50}}} = 1.35 \log\left(15\frac{h}{D_{50}}\right) \qquad (5)$$

to determine the size of riprap round bridge piers in which $U_{max} = 1.2\ U_0$, Δ is the submerged specific density of the riprap, and g is the acceleration due to gravity. Equation 5 is transcendental and has to be solved by iteration although convergence is very fast. Croad noted the Equation 5 was not always conservative in its estimate of the riprap size.

Croad (1990) also presented an alternative formula based on applying the scour prediction formula of Melville and Sutherland (1987) in reverse to determine the riprap size D required to limit the scour depth to D (i.e. riprap size). This leads to estimates for the required riprap size which are often significantly larger than that actually required.

Table 1.3 Summary of experimental data from Croad (1990).

Run	Bed d_{50} (mm)	Riprap D_{50} (mm)	Pier type	d_s (m)	U_{0max} (m/s)	Performance
1	2.2	–	slab	0.089	0.51	severe scour
2	2.2	19.8	slab	0.045	0.61	stable
3	2.2	11.0	slab	0.062	0.58	stable
4	2.2	7.7	slab	0.068	0.62	stable
5	2.2	7.7	slab	large	0.62	severe scour
6	7.7	11.0	cylinder	0.036	0.94	moderate scour
7	7.7	11.0	cylinder	0.048	0.87	moderate scour
8	7.7	12.7	cylinder	0.028	0.91	moderate scour
9	7.7	12.7	slab	0.046	0.73	severe scour
10	7.7	12.7	slab	0.043	1.01	stable
11	7.7	12.7	slab	0.032	0.98	moderate scour
12	7.7	15.8	slab	0.044	1.04	stable

Several of the cases in Table 1.3 show quite different performances even though the basic conditions (e.g. bed size, riprap size) are the same. No specific explanation can be offered for this. It will be observed later that there is a large amount of scatter in the data anyway and that recommended design formulae should form a lower bound (conservative) envelope to the data.

Since the preparation of the initial draft of this report, two studies have been published. The first is that by Parola (1993) who carried out a review of existing formulae and conducted experiments for rectangular and circular piers. From these experiments, for rectangular piers, Parola (1993) recommended:

$$\frac{U_0}{\sqrt{\Delta g D_{50}}} \leq 0.9 \qquad \text{for} \quad 20 < \frac{b}{D} < 33$$

$$\frac{U_0}{\sqrt{\Delta g D_{50}}} \leq 1.0 \qquad \text{for} \quad 7 < \frac{b}{D} < 14 \tag{6}$$

$$\frac{U_0}{\sqrt{\Delta g D_{50}}} \leq 1.1 \qquad \text{for} \quad 4 < \frac{b}{D} < 7$$

Parola (1993) placed the riprap in three layers and defined the critical conditions as being the point where the second or middle layer was (incipiently) undisturbed. For circular piers, Parola (1993) recommended that:

$$\frac{U_0}{\sqrt{\Delta g D_{50}}} \leq 1.18 \tag{7}$$

For Parola's experiments, the riprap to sediment size ratios were in the range $0.2 \leq D/d < 13$ and experiments were for non-sediment transport (i.e. clear water scour) conditions. Parola found that the most critical conditions occurred when the riprap was placed slightly below the bed level. He also concluded that, for a given rock size, the critical velocity reduced with increasing depth of flow when the riprap was exposed above the bed, but was relatively insensitive to this effect when the riprap was only exposed at or was below the bed level.

The second experimental study was reported by Chiew (1996) on riprap that was set flush with the bed. For critical conditions, Chiew concluded that the stone size should be given by:

$$D_{50} \geq \frac{U_0^3}{10.47\sqrt{h}} \tag{8}$$

where D_{50}, U_0 and h are given in units of m, m/s and m respectively. Chiew's experiments were based on riprap (D) to bed sediment (d) ratios of $2.7 < D_{50}/d_{50} < 5$, water depth (h) to pier diameter (b) ratios of $2 < h/b < 8.6$. All experiments were confined to circular piers.

Chiew (1996) concluded that the threshold of pier scour around a circular pier occurs when the mean flow velocity exceeds 0.3 times the critical flow velocity for the bed sediment. Chiew also concluded that winnowing can significantly affect the efficiency of a riprap layer (i.e. the riprap layer may submerge into the scour hole), even though the riprap layer may remain intact.

2. EXPERIMENTAL STUDIES

2.1 General

Two test rigs were used at Opus for a total of 32 experiments to carry out the study reported here.

Task 1 involved studying isolated piers with different flow velocities and bed sediment sizes. Task 2 tested two adjacent piers, and a pier adjacent to an abutment, with different flow velocities and bed sediment sizes. The experiments reported in Croad (1990) involved clear water scour conditions (i.e. no general bed sediment transport), whereas these studies involved both general sediment transport and degrading bed conditions.

2.2 Tilting Flume Studies

Task 1 was carried out in a tilting steel and glass flume (Figure 2.1a) measuring 22.0 m long by 0.45 m wide by 0.45 m high. Water was supplied to the flume from the laboratory constant head tank system using one inflow line. Water levels were controlled by an adjustable tail gate.

A false floor was installed in the flume which extended some 10.0 m upstream of the working section. The false floor had a stone-roughened surface to ensure that the velocity profile adapted to a constant, more or less logarithmic, velocity profile at the working section after the transition to the false floor. Measured vertical velocity profiles are shown in Figure 2.2.

$$\frac{u}{u_*} = \frac{1}{\kappa} \ln\left(\frac{y}{k}\right) + B \qquad (9)$$

The straight lines on the log-normal plots confirm that the profiles conform to the relationship given by Equation 9 in which:

- y = height above the bed,
- u = velocity at height y,
- u_* = $\sqrt{(\tau/\rho)}$ = shear velocity,
- τ = bed shear stress,
- ρ = density of water,
- κ = 0.4 = von Karmen constant,
- k = roughness height, and
- B = a constant.

All velocity measurements were made using a Streamflow miniature velocity propeller meter (serial No. 405/8999) with a propeller diameter of 5 mm. The velocity probe was calibrated in a special purpose annular flume. The accuracy of the probe was considered to be ± 2%.

Figure 2.1 Views of the flumes used in the experimental programme.

(a) Tilting flume looking towards tail gate.

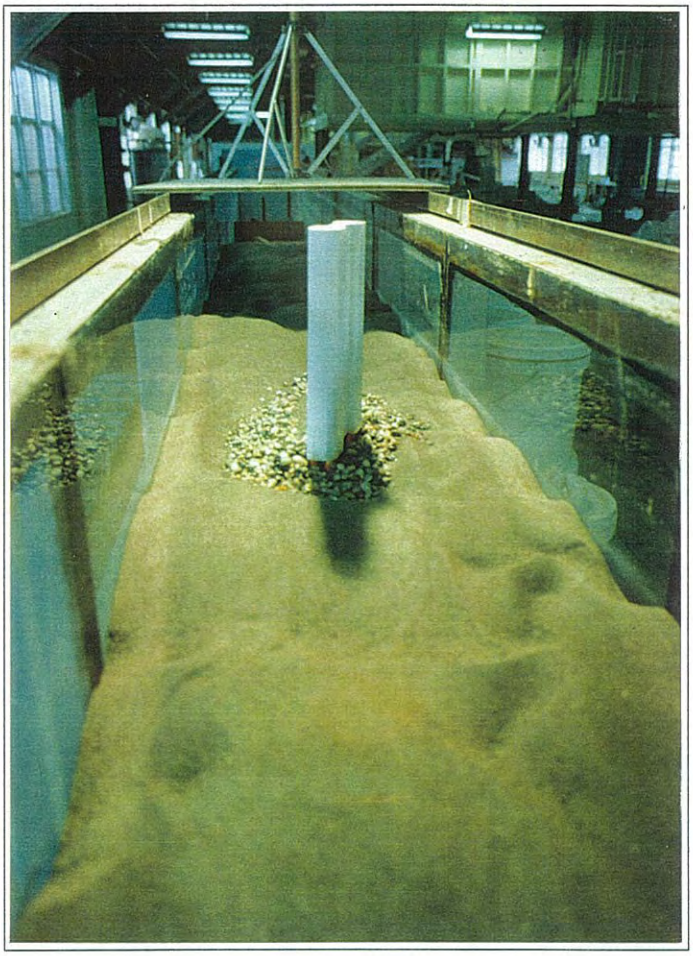

(b) Wide flume looking from tail gate (below bottom margin of photograph).

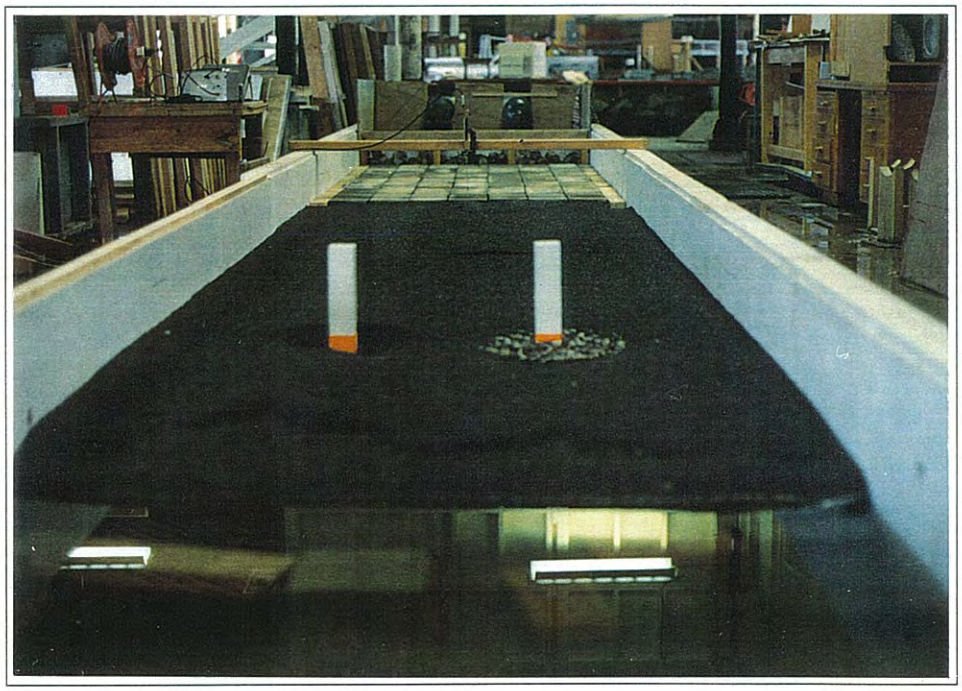

Flow rates were measured using an Emflux 150 mm diameter electromagnetic flow meter (serial No. 1870 with amplifier and range unit serial No. 1676). The flow meter was calibrated in the laboratory's volumetric calibration tank to an accuracy of ±1%.

Figure 2.2 Vertical velocity profiles measured in the tilting flume for isolated piers.

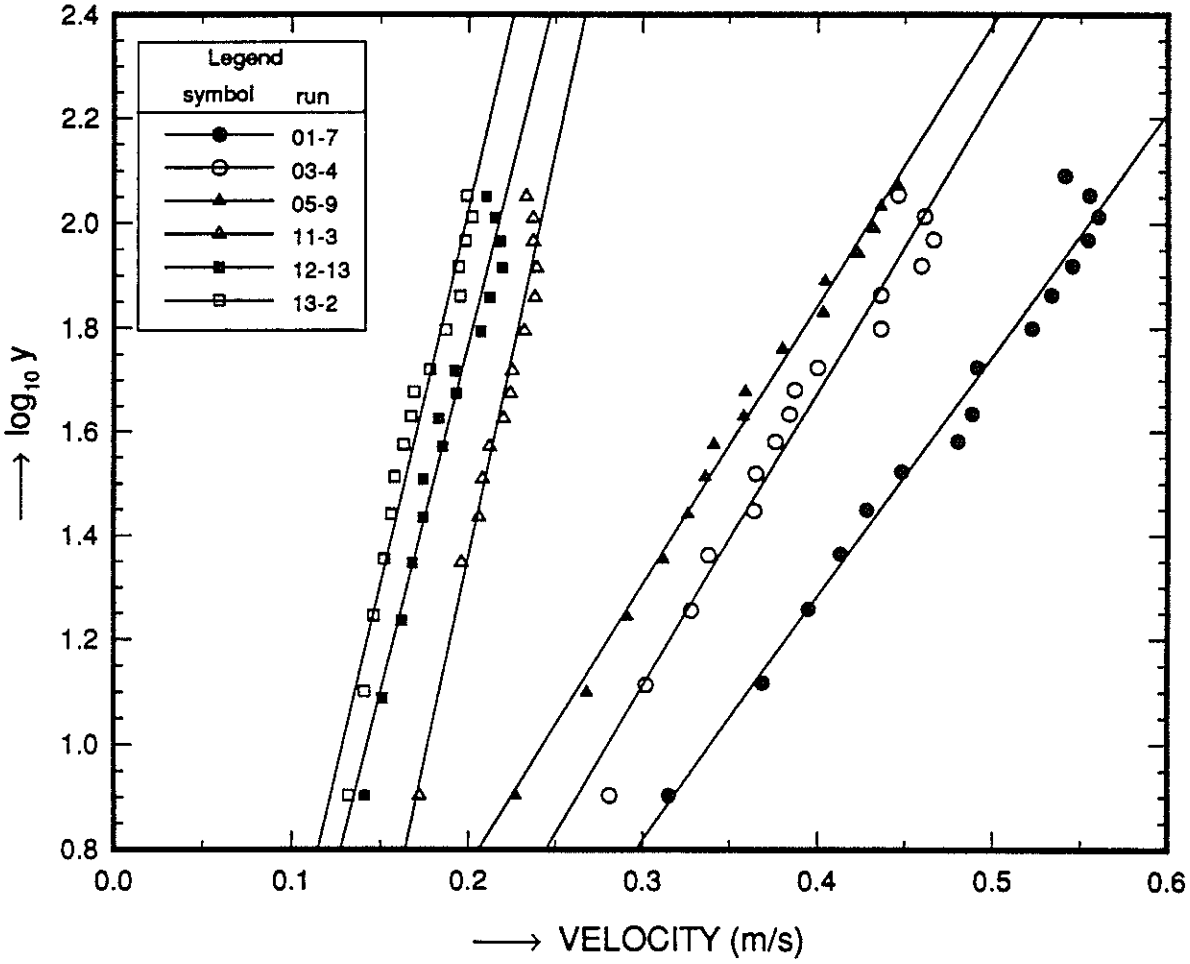

2.3 Wide Flume Studies

Task 2 was carried out in a wide wooden flume measuring 12.0 m long by 1.5 m wide by 0.4 m high (Figure 2.1b). Water was supplied from the laboratory's constant head tank supply system using two inflow lines. Water levels were controlled using an adjustable flap tail gate (not shown on Figure 2.1b).

A false floor constructed of 0.19 m high masonry blocks extending some 5.0 m upstream of the working section was used. Water passed through a stone baffle before entering the flume to provide a velocity profile which was uniform across the width of the flume.

Velocities in this flume were measured using the same instruments and methodologies as employed in the tilting flume.

2.4 Bed Sediment and Riprap Properties

Two sizes of bed sediment and two sizes of riprap were used in the study as specified in Table 2.1. The geometric standard deviation σ_g is defined to be $\sigma_g = d_{85}/d_{50}$.

Table 2.1 Properties of bed sediments and riprap used in experiments.

Application	Median size (mm)	Geometric standard deviation
bed sediment (d)	$d_{50} = 2.20$ $d_{50} = 0.29$	1.2 1.9
riprap (D)	$D_{50} = 8.00$ $D_{50} = 15.0$	1.5 1.4

2.5 Pier Shapes

Four pier shapes were used, and their appearance and arrangement are shown in Figures 2.4 to 2.35:

1. Circular - 60.5 mm diameter.
2. Square - 60.0 mm side length.
3. Slab pier type 1 (T1) - 166 mm long by 23 mm wide at the base. This pier is typical of the slender slab pier built before 1960, supported on six (but often more) octagonal concrete piles. The particular design used here is the same as used by Croad (1990) and is based on the Waingawa bridge where SH2 crosses the Waingawa River near Masterton.
4. Slab pier type 2 (T2) - 170 mm long by 38 mm wide. This pier is thicker than type 1, and incorporates twelve piles, ten of which form two clusters of five at each end of the slab. The dimensions used here were based on the Matawhero bridge near Gisborne given in Melville (1975). In some of the later experiments, dacron was wrapped around the piles to simulate the effects of debris clogging the piles.

Although the results from these experiments are presented in dimensionless form, the dimensions of the piers used in the experiments correspond to a scale of 1:40, relative to the prototype structures on which they were modelled. The depths of water (i.e. 0.075–0.15 m) used in the experiments, therefore, corresponded to 3–6 m which is a realistic range of depths to consider for floods in New Zealand rivers.

For the tests carried out in the wide flume, the spacing between piers was 0.4 m measured centre to centre. This distance is approximately 16 m in the prototype structures and is representative of many bridges built during the 1940-70 era. The spacing used between the abutment and pier was also 4.0 m for experiments that

involved these two elements. Pier spacing and abutment–pier spacing were not examined as a variable within the range of tests planned within the experimental programme.

For experiments involving two piers, riprap was placed around one of the piers only. Where a skewed alignment was used it was placed around the downstream pier. The other pier was allowed to scour freely. This arrangement was considered to represent a more severe test of the riprap layer, as the scour hole often extended to the edge of the riprap layer causing its edge to lower and perhaps unravel.

2.6 Plan Dimensions of Riprap

The riprap extended a distance B_f in front of the pier, B_s to either side, and had an overall length of B_L in the direction of flow, as defined in Figure 2.3. The values for B_f, B_s and B_L adopted in the different experiments are given in Tables 2.2 and 2.3.

2.7 Use of Filter Layer

Filter material was sometimes used over the fine sediment beneath the riprap as indicated in Tables 2.2 and 2.3. The filter material consisted of a widely graded sediment with a median diameter of 2.2 mm. A thickness equivalent to the median size of the overlying riprap was used and covered the area indicated in Figure 2.3.

2.8 Test Procedures

Task 1 experiments

For the Task 1 experiments carried out in the tilting flume, the pier and riprap was installed to the required geometry. The flume was slowly flooded with water up to the required water level. The flow was then started and increased in increments at 0.5 hour intervals. The velocity was increased incrementally until the riprap mat had completely disintegrated or (less commonly) the maximum flow that was possible with the laboratory head tank supply was achieved.

Up to 12 increments in velocity were involved in each experiment. At the end of each flow sequence the flow was stopped and the pier and riprap were photographed. Measurements of the depth of scour in, or lowering of the surface of, the riprap mat were also made.

Measurements of the scour depth around the piers without riprap in place were also carried out for runs 1, 3, 6 and 7 (corresponding to the first use of the different pier shapes). This allowed the velocity to be determined at which initial scour occurred around the piers.

Figure 2.3. Plan layout of the riprap and filter layers around two types of pier.

(a) Square pier

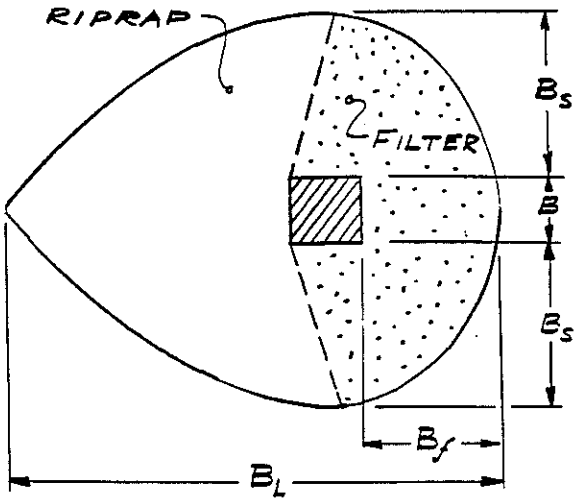

B = pier size

(b) Slab pier

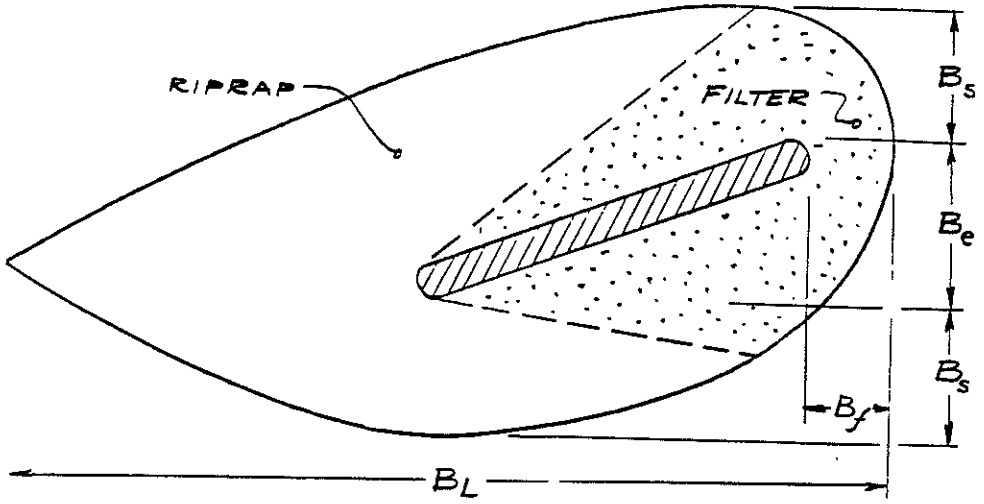

(c) Representative cross-section view of a slab pier.

t = thickness of riprap mat

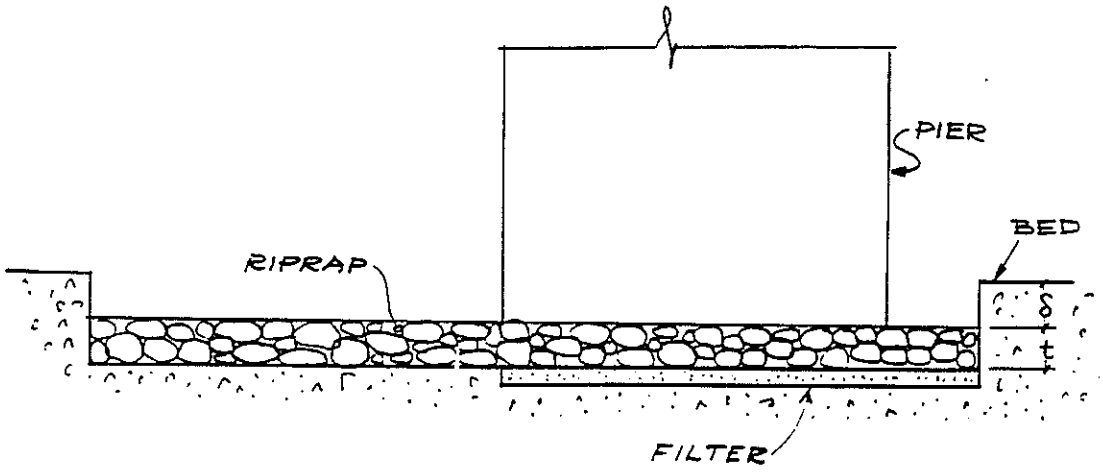

(See Section 2.9 for explanation of other symbols)

Task 2 experiments

The procedures used in the Task 2 experiments carried out in the wide flume were very similar to those used in Task 1 except that, generally, fewer increments in velocity were used because the expected performance of the riprap could be anticipated by this Task 2 stage.

In all the experiments, three criteria were used, all three of which had to be met, to define a threshold of satisfactory performance for the riprap mat. They were:

1. The maximum depth of lowering of the riprap mat around the pier (including any local scour) should not exceed 0.05 m (equivalent to approximately 2 m in prototype terms).
2. The riprap mat should remain largely intact. However, some ravelling leading to loss of riprap from the downstream edge of the mat was tolerated.
3. Any local scour in the riprap adjacent to the pier should not penetrate through the riprap mat that would expose the underlying filter layer (if present) or bed sediment.

2.9 Results

The measured data from the experiments and other relevant information are presented in Tables 2.2 and 2.3. Figures 2.4 to 2.35 show the pier and riprap corresponding to the last sub-run at which the riprap mat was still intact (i.e. the run before failure according to the criteria given in Section 2.8). In two cases the riprap layer failed to perform, or showed signs of severe distress, right from the outset. These cases are marked "failed" or "damaged" in the tables. The following symbols are used in Tables 2.2 and 2.3:

d_{50}	Median size (mm) of the bed sediment
D_{50}	Median size (mm) of the riprap
α	Angle in degrees of the pier to the approach flow
θ	Angle in degrees of the bridge centre line to the direction at right angles to the river (or flume)
h	Upstream water depth (mm)
δ	Depth (mm) to the top of the riprap from the initial bed level (setdown)
d_s	Maximum depth (mm) of scour over the riprap mat measured from the surface of the mat
B_f	Extent (mm) of riprap mat in front of pier (Figure 2.3)
B_e	Effective width of slab pier (Figure 2.3)
B_s	Lateral extent (mm) of riprap mat (Figure 2.3)
B_L	Overall length (mm) of riprap mat in the flow direction (Figure 2.3)
U_0/U_{0c}	Ratio of upstream velocity to critical velocity corresponding to incipient scour at the pier
$U_{0,max}$	Maximum upstream approach velocity for which the riprap mat performed satisfactorily (corresponding to the state shown in Table 2.3)

The following observations are made:

1. For Runs 24, 30, 31 and 32 the reference velocity $U_{0,max}$ was measured between the abutment and the pier. This was done after the failure of the riprap mat in Run 23 (also involving an abutment) when it was apparent that the contracted flow velocity caused by the abutment, rather than the upstream approach velocity, was the more relevant velocity to consider.

2. Scour was usually initiated at the sides of the piers. For the circular and square shapes, scour then progressed towards the front of the piers. For the slab piers, the larger scour depths then tended to shift towards the downstream side of the pier.

3. For failure of the fine bed sediment, the riprap layer lowered around the outside of the mat as the bed degraded but the layer usually remained intact. For coarse bed sediment, failure tended to be very rapid once started, because the riprap stones rolled away.

4. The riprap mat tended to suffer more damage or disturbance as the troughs of the dunes in the mobile bed sediment passed over the riprap mats.

   No systematic measurements of dune heights were made as dune height was variable from dune to dune, especially in finer bed sediments. Accurate measurement of dune properties requires a statistical approach based on many dunes. Also, the bridge piers, and the effects of the wake from the piers, tended to distort the dunes as they passed through. In the fine bed sediment, the dunes were also usually covered in smaller ripples. Although the ripples were present in the experiments, they are not representative of what typically occurs in prototype rivers. Ripples will not be present in rivers with coarse sand and gravel beds.

   However, by observation, dunes were roughly 0.02-0.05 m in amplitude which corresponds to approximately 0.8-2 m in the prototype. The front edges of dunes can be seen in some of the Figures.

5. No interaction between adjacent piers affected the riprap stability, even when the centre line of the bridge was aligned at 30° to the normal to the flow direction. The interaction between a pier and an adjacent abutment was very important, however, because of the effect of contracted flow velocity.

6. The use of a filter layer under the upstream part of the riprap mat improved the performance of the protection system and generally prevented the burying of the riprap stones into underlying sediment.

7. The wider riprap mats, corresponding to about two times the effective width of the pier, appeared to be more stable, and to cope with large deformations in the bed caused by general bed lowering and the progression of sediment dunes past the pier.

8. Several of the Figures show only a limited amount of the riprap, which gives the impression that the mat has disintegrated. Inspection at the time, however, verified that the mat had simply been covered by bed sediment.

Table 2.2 Summary of experimental data from Task 1 tilting flume experiments.

Run	Pier		Bed Sediment d_{50} (mm)	Riprap D_{50} (mm)	Riprap Mat Dimensions			Filter	h (m)	U_0/U_{0c}	δ (mm)	d_s (m)	$U_{0,max}$ (m/s)
	Type	α			B_f (mm)	B_s (mm)	B_L (mm)						
1	circular		2.2	8.0	45	60	285		0.15	0.45	0	0.020	0.54
2	circular		2.2	15.0	45	60	285		0.15		0	0.060	0.84
3	square		2.2	2.2	-	-	-		0.15	0.35	0	0	0.19
4	square		2.2	8.0	60	80	360		0.15		0	0.015	0.48
5	square		2.2	15.0	60	80	360		0.15		0	0.075	0.75
6	slab T1	20	2.2	8.0	50	60	470		0.15	0.49	0	0.043	0.64
7	slab T1	20	2.2	15.0	50	60	470		0.15	0.45	0	0.045	0.87
8	slab T2	20	2.2	15.0	50	75	450		0.15		0	0.055	0.85
9	slab T2	20	2.2	8.0	50	75	450		0.15		0	0.052	0.64
10	slab T2	20	0.29	8.0	50	75	450		0.15		15	0.025	0.55
11	slab T2	20	0.29	8.0	50	75	450		0.15		25	0.050	0.81
12	square		0.29	8.0	60	80	360		0.15		25	0.070	0.56
13	square		0.29	15.0	60	80	360		0.15		25	0.080	0.82
14	square		0.29	15.0	120	160	450		0.15		25	0.050	0.82
15	slab T2	20	0.29	15.0	120	160	450		0.15		25	0	0.82
16	square		2.2	15.0	120	150	450	✓	0.15		25	0	0.82

Explanation of symbols used in Figure 2.3, Tables 2.2, 2.3

- d_{50} Median size (mm) of the bed sediment
- D_{50} Median size (mm) of the riprap
- α Angle in degrees of the pier to the approach flow
- θ Angle in degrees of the bridge centre line to the direction at right angles to the river (or flume)
- h Upstream water depth (mm)
- δ Depth (mm) to the top of the riprap from the initial bed level (setdown)
- d_s Maximum depth (mm) of scour over the riprap mat measured from the surface of the mat
- B_f Extent (mm) of riprap mat in front of pier (see Figure 2.3)
- B_s Lateral extent (mm) of riprap mat (see Figure 2.3)
- B_L Overall length (mm) of riprap mat in the flow direction (see Figure 2.3)
- U_0/U_{0c} Ratio of upstream velocity to critical velocity corresponding to incipient scour at the pier
- $U_{0,max}$ Maximum upstream approach velocity for which the riprap mat performed satisfactorily (corresponding to the state shown in Table 2.3)

Table 2.3 Summary of experimental data from Task 2 wide flume experiments.

Run	Pier			Bed Sediment d_{50} (mm)	Riprap D_{50} (mm)	Riprap Mat Dimensions			Filter	h (m)	δ (mm)	Debris	d_s (m)	$U_{0,max}$ (m/s)
	Type	α	θ			B_f (mm)	B_s (mm)	B_L (mm)						
17	2 piers (square)		0	2.2	15.0	120	150	450		0.10	25		0.01	1.20
18	2 piers (square)		0	2.2	8.0	120	150	450		0.10	25		0	0.50
19	2 slab piers T2	20	0	2.2	8.0	120	160	450		0.10	25		0.05	0.85
20	2 slab piers T2	20	0	2.2	15.0	120	160	450		0.10	25		0.04	1.00
21	2 slab piers T2	30	0	2.2	8.0	120	160	550		0.15	25	✓	0	0.49
22	2 slab piers T2	30	0	2.2	15.0	120	160	550		0.15	25	✓	0	0.67
23	slab T2 & abutment	30	30	2.2	8.0	120	160	550		0.075	25	✓	failed	0.41
24	slab T2 & abutment	30	30	2.2	15.0	120	160	550		0.075	25	✓	0	0.96
25	2 slab piers T2	30	30	0.29	15.0	120	160	550	✓	0.075	25	✓	0	0.48
26	2 slab piers T2	30	30	0.29	8.0	120	160	550	✓	0.075	25	✓	0	0.41
27	2 slab piers T2	30	30	0.29	8.0	120	160	550	✓	0.075	25	✓	0	0.41
28	2 slab piers T2	30	30	0.29	15.0	120	160	650	✓	0.075	25	✓	0	0.48
29	slab T2 & abutment	30	0	0.29	8.0	120	160	650	✓	0.075	25	✓	damaged	0.41
30	slab T2 & abutment	30	0	0.29	8.0	120	160	650	✓	0.075	25	✓	0	0.41
31	slab T2 & abutment	30	0	0.29	15.0	120	160	650	✓	0.075	25	✓	0	0.41
32	slab T2 & abutment	30	30	0.29	15.0	120	160	650	✓	0.075	25	✓	0	0.41

(See Table 2.2 for explanation of symbols)

Tilting Flume Experiments
(Figures 2.4 to 2.19)

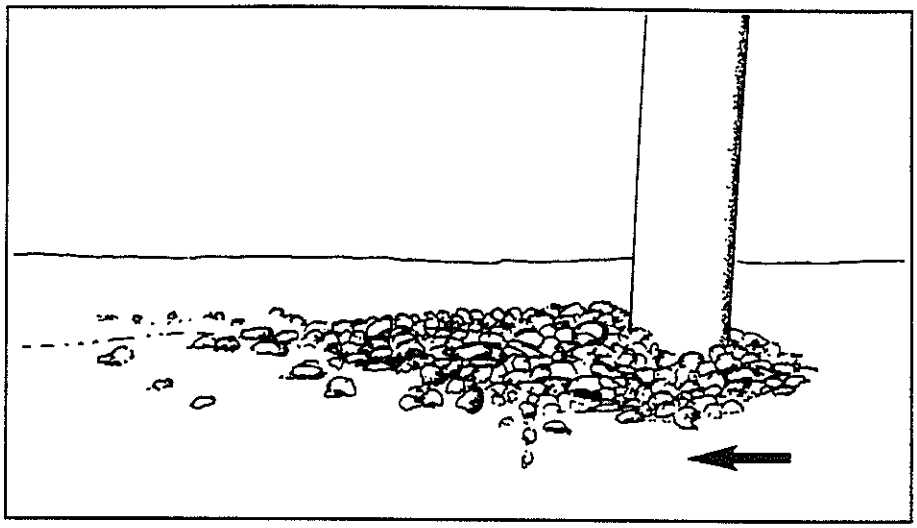

Figure 2.4 Run 1
Circular pier, $\alpha = 0°$;
flow –; $D_{50} = 8$ mm;
$U_{o,max} = 0.54$ m/s

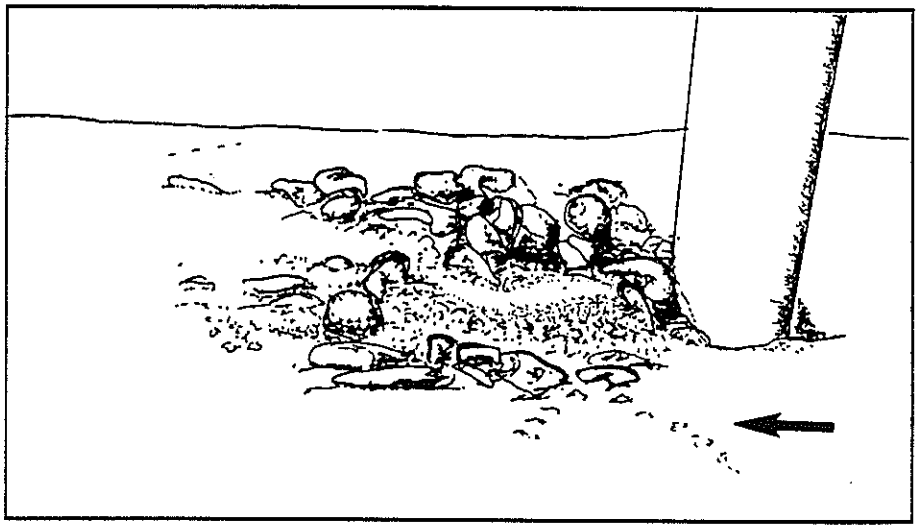

Figure 2.5 Run 2
Circular pier, $\alpha = 0°$;
flow –; $D_{50} = 15$ mm;
$U_{o,max} = 0.84$ m/s

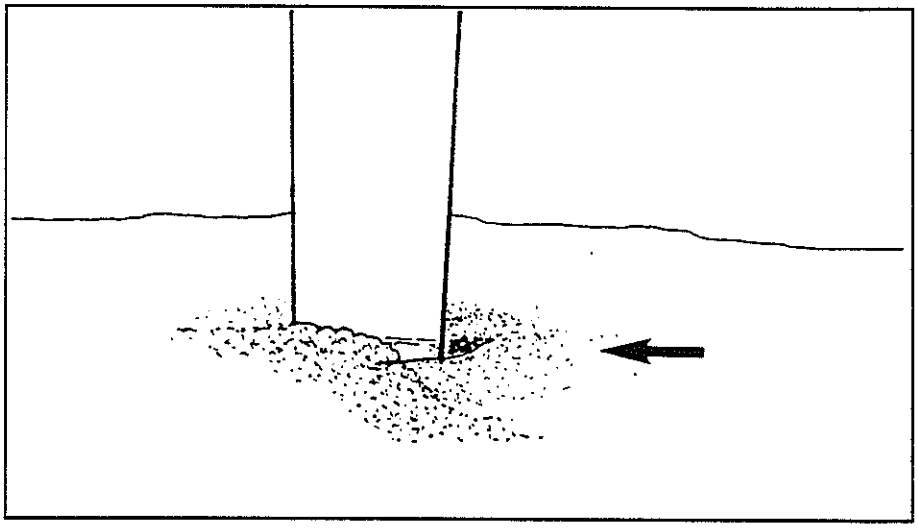

Figure 2.6 Run 3
Square pier, $\alpha = 0°$;
flow –; $D_{50} = 2.2$ mm;
$U_{o,max} = 0.19$ m/s

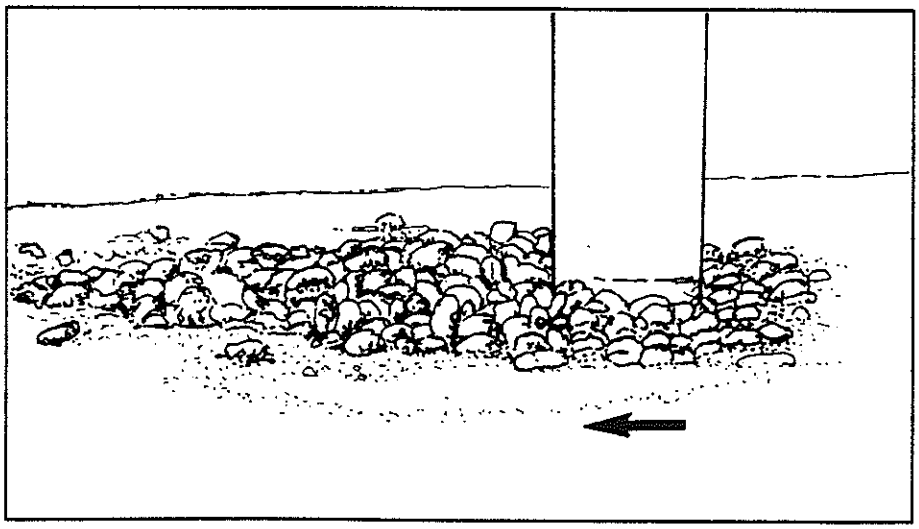

Figure 2.7 Run 4
Square pier, $\alpha = 0°$;
flow –; $D_{50} = 8$ mm;
$U_{o,max} = 0.48$ m/s

(Drawings copied from photographs)

Figure 2.8 Run 5
Square pier, $\alpha = 0°$;
flow ←; $D_{50} = 15$ mm;
$U_{o,max} = 0.75$ m/s

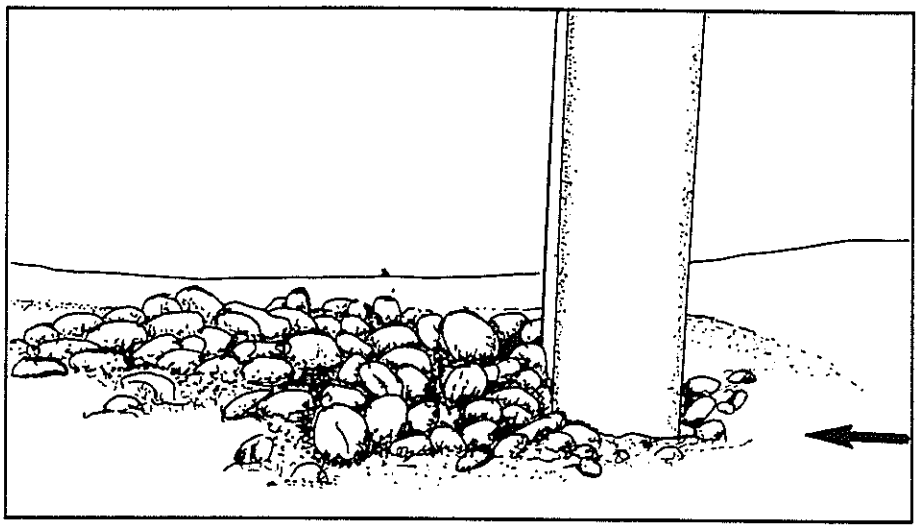

Figure 2.9 Run 6
Slab pier T1, $\alpha = 20°$;
flow →; $D_{50} = 8$ mm;
$U_{o,max} = 0.64$ m/s

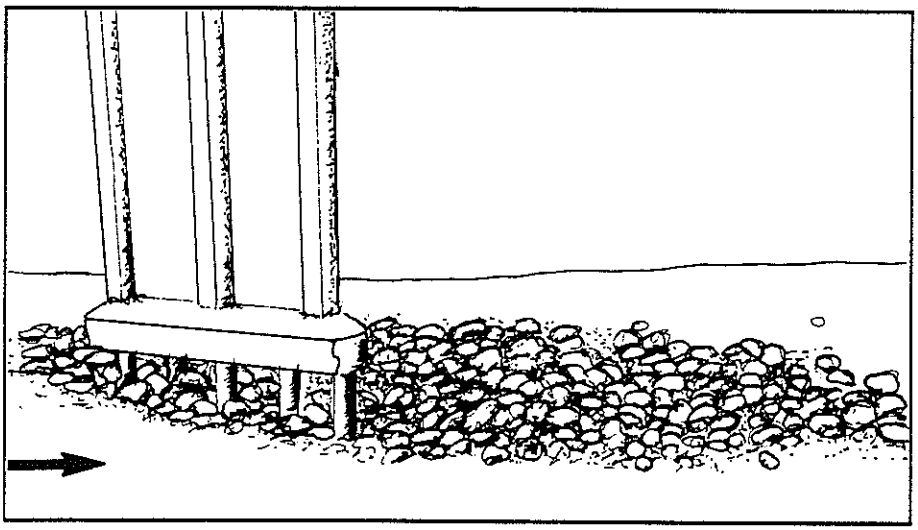

Figure 2.10 Run 7
Slab pier T1, $\alpha = 20°$;
flow →; $D_{50} = 15$ mm;
$U_{o,max} = 0.87$ m/s

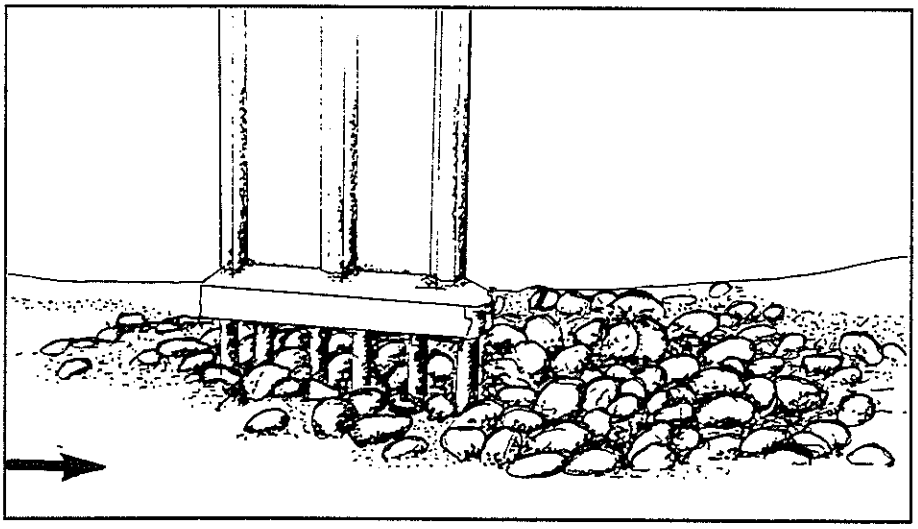

Figure 2.11 Run 8
Slab pier T2, $\alpha = 20°$;
flow ←; $D_{50} = 15$ mm;
$U_{o,max} = 0.85$ m/s

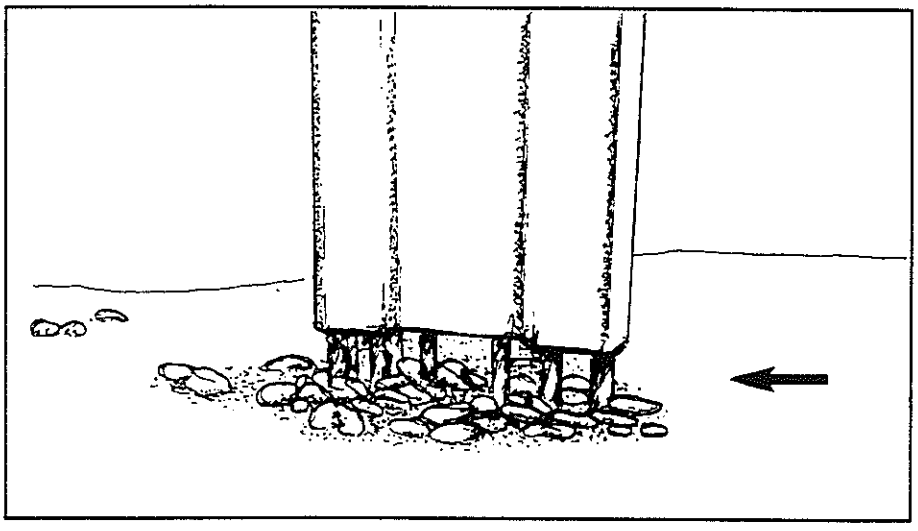

(Drawings copied from photographs)

Figure 2.12 Run 9
Slab pier T2; $\alpha = 20°$;
flow ←; $D_{50} = 8$ mm;
$U_{o,max} = 0.64$ m/s

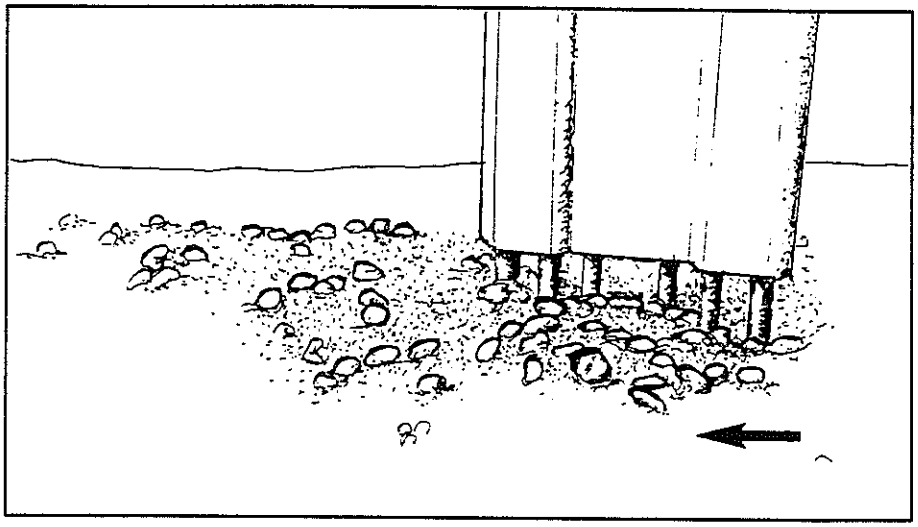

Figure 2.13 Run 10
Slab pier T2; $\alpha = 20°$;
flow ←; $D_{50} = 8$ mm;
$U_{o,max} = 0.55$ m/s

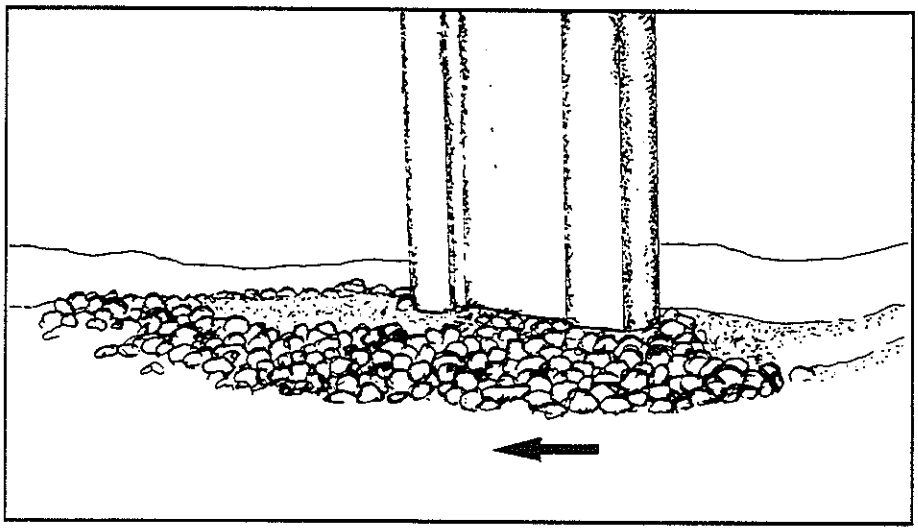

Figure 2.14 Run 11
Slab pier T2; $\alpha = 20°$;
flow →; $D_{50} = 8$ mm;
$U_{o,max} = 0.81$ m/s

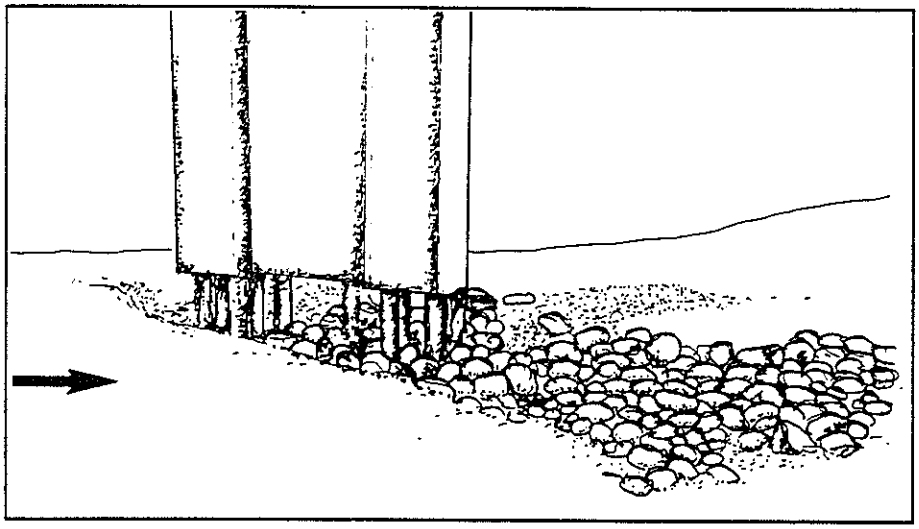

Figure 2.15 Run 12
Square pier; $\alpha = 0°$;
flow ←; $D_{50} = 8$ mm;
$U_{o,max} = 0.56$ m/s

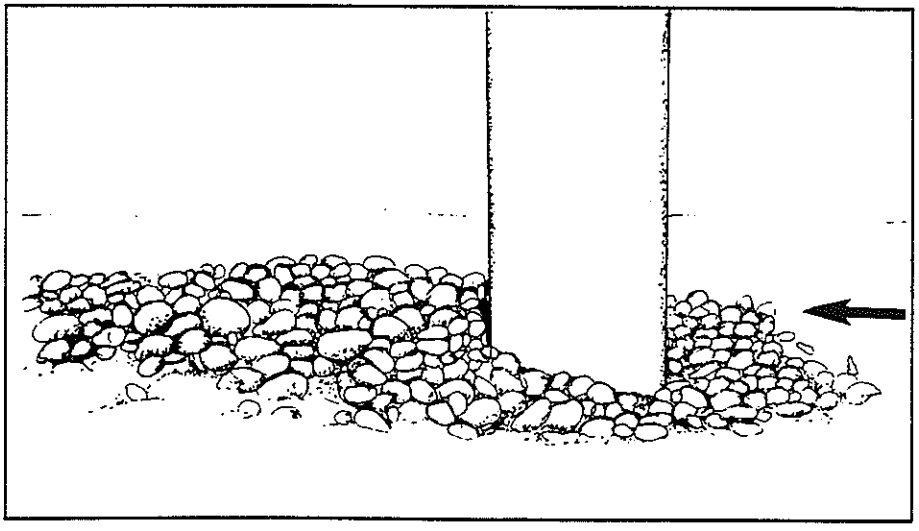

(Drawings copied from photographs)

Figure 2.16 Run 13
Square pier: $\alpha = 0°$;
flow ←; D_{50} = 15 mm;
$U_{o.max}$ = 0.82 m/s

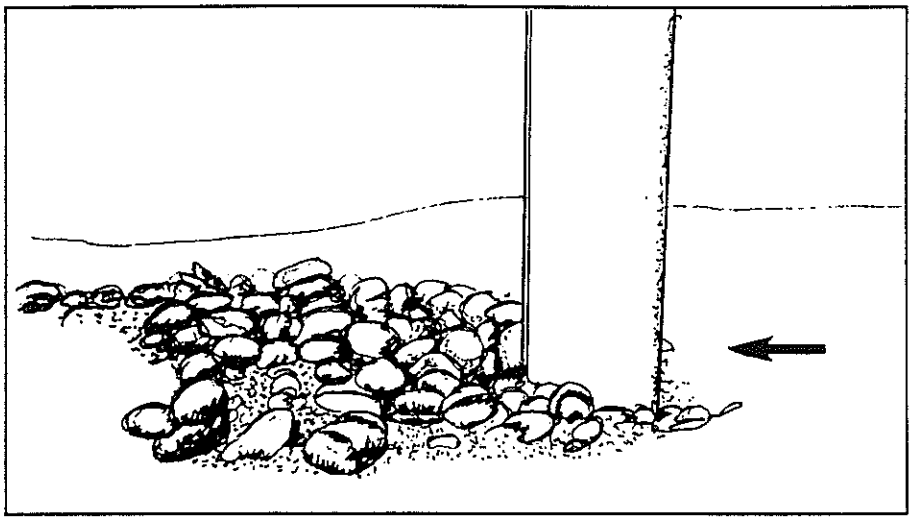

Figure 2.17 Run 14
Square pier: $\alpha = 0°$;
flow ←; D_{50} = 8 mm;
$U_{o.max}$ = 0.82 m/s

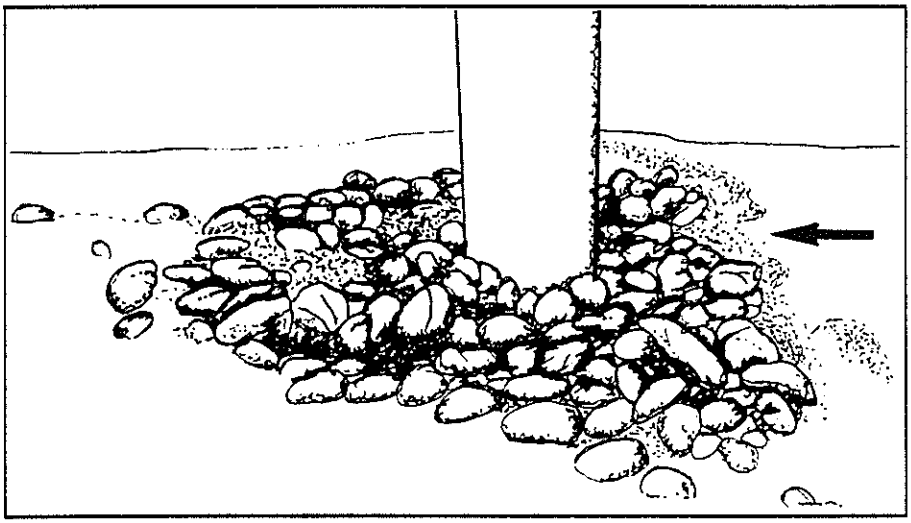

Figure 2.18 Run 15
Slab pier T2, $\alpha = 20°$;
flow ←; D_{50} = 15 mm;
$U_{o.max}$ = 0.82 m/s

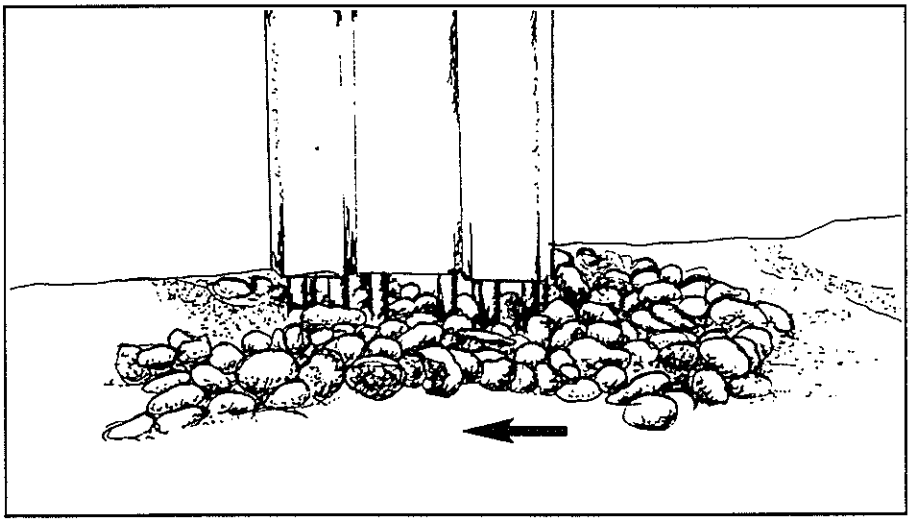

Figure 2.19 Run 16
Square pier: $\alpha = 0°$;
flow →; D_{50} = 15 mm;
$U_{o.max}$ = 0.82 m/s

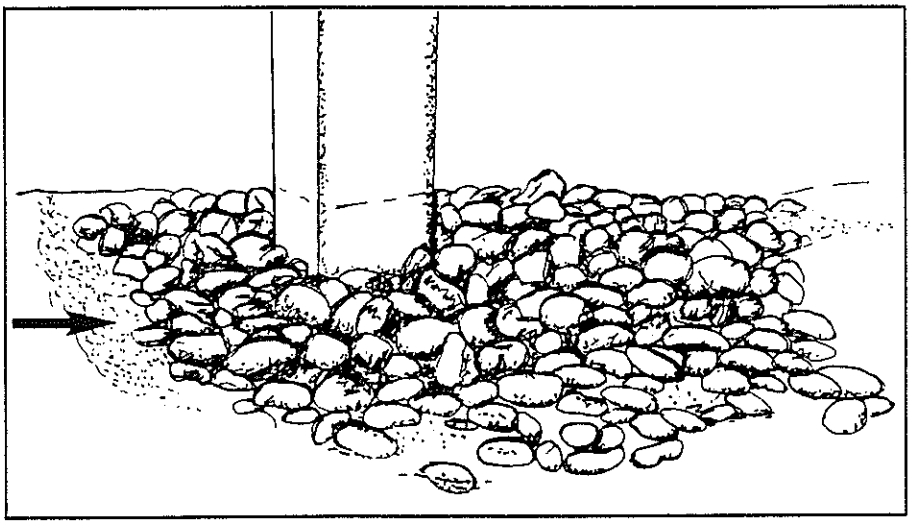

(Drawings copied from photographs)

Wide Flume Experiments
(Figures 2.20-2.32)

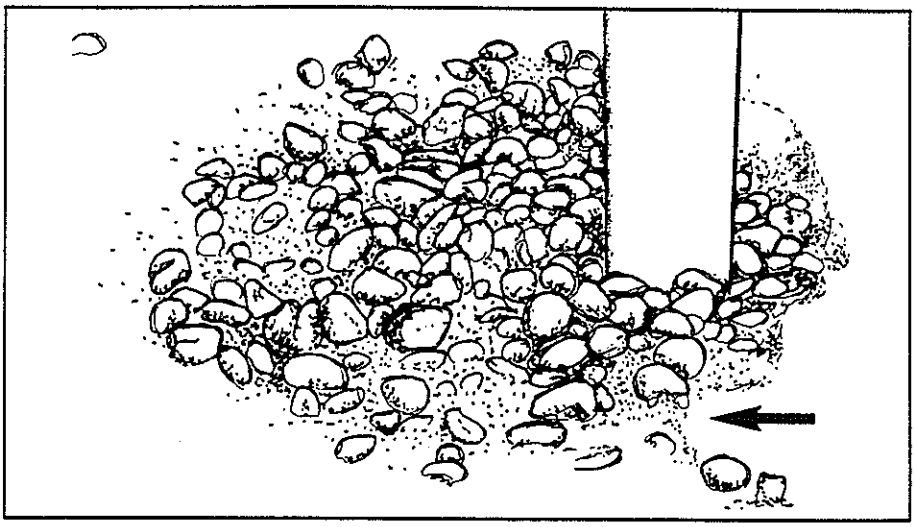

Figure 2.20 Run 17
Square piers (second pier out of frame); $\alpha = 0°$;
flow ←; D_{50} = 15 mm;
$U_{o,max}$ = 1.20 m/s

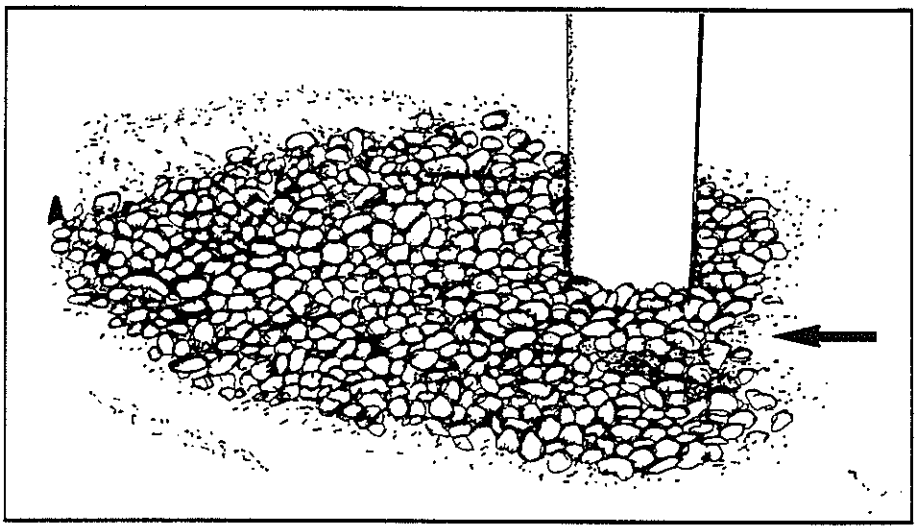

Figure 2.21 Run 18
Square piers (second pier out of frame); $\alpha = 0°$;
flow ←; D_{50} = 8 mm;
$U_{o,max}$ = 0.50 m/s

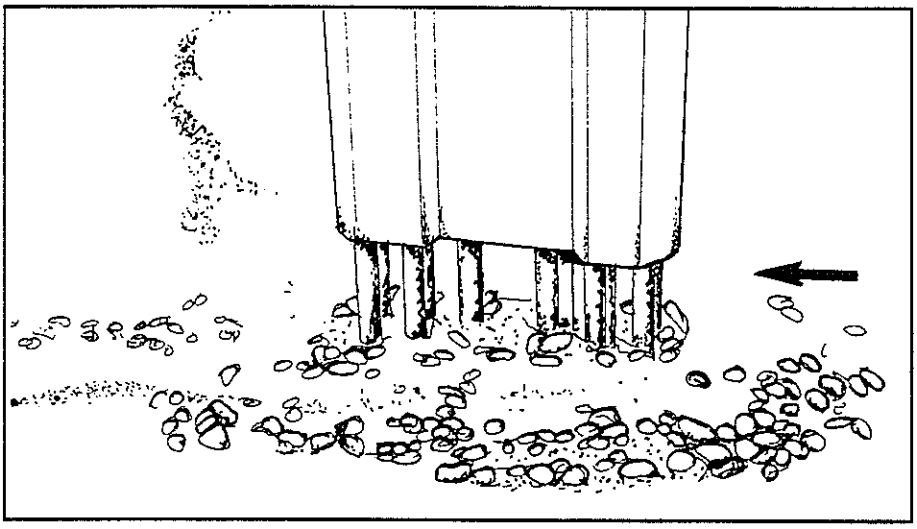

Figure 2.22 Run 19
Slab piers T2 (second pier out of frame); $\alpha = 20°$;
flow ←; D_{50} = 8 mm;
$U_{o,max}$ = 0.85 m/s

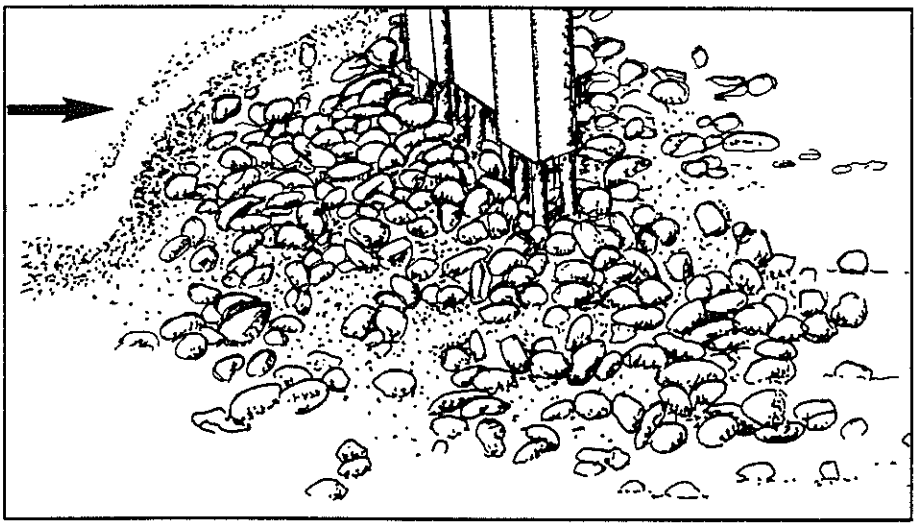

Figure 2.23 Run 20
Slab piers T2 (second pier out of frame); $\alpha = 20°$;
flow →; D_{50} = 15 mm;
$U_{o,max}$ = 1.00 m/s

(Drawings copied from photographs)

Figure 2.24 Run 21
Slab piers T2; $\alpha = 30°$;
flow ←; $D_{50} = 8$ mm;
$U_{o,max} = 0.49$ m/s

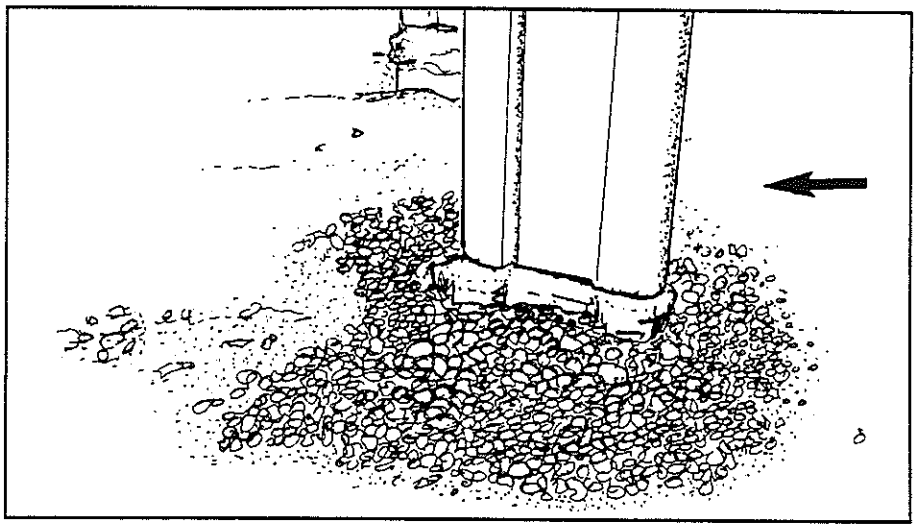

Figure 2.25 Run 22
Slab piers T2 (second pier collapsed from scour);
$\alpha = 30°$; flow ←;
$D_{50} = 8$ mm;
$U_{o,max} = 0.67$ m/s

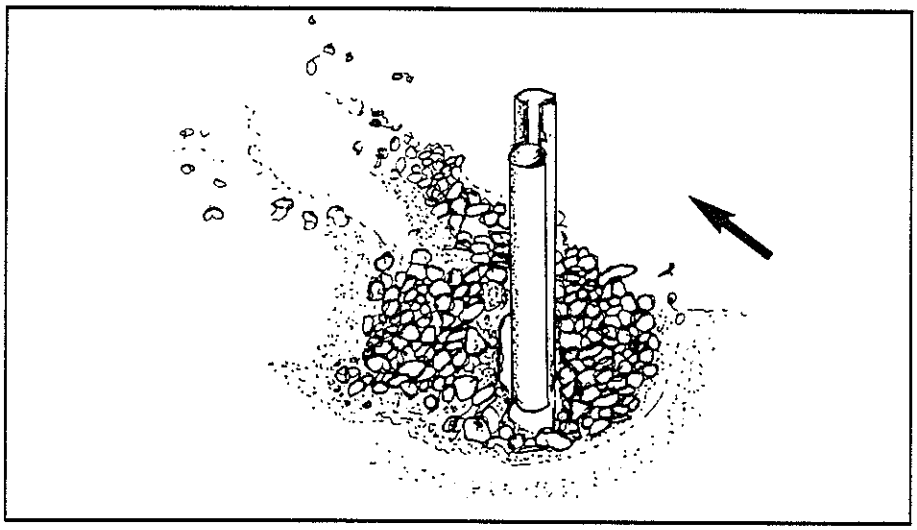

Figure 2.26 Run 23
Slab pier T2 + abutment;
$\alpha = 30°$; flow →;
(riprap completely scoured from upstream edge, on abutment side of pier);
$D_{50} = 8$ mm;
$U_{o,max} = 0.41$ m/s

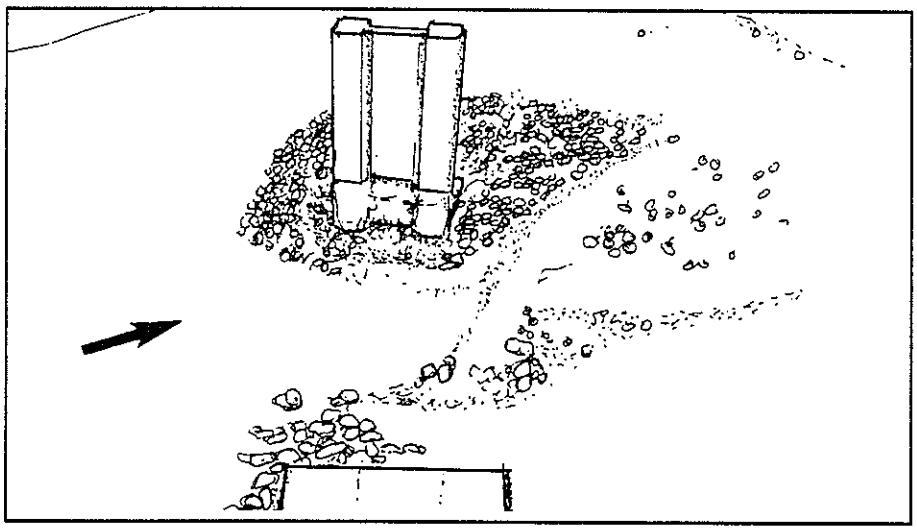

Figure 2.27 Run 24
Slab pier T2 + abutment;
$\alpha = 30°$; flow ↖;
$D_{50} = 15$ mm;
$U_{o,max} = 0.96$ m/s

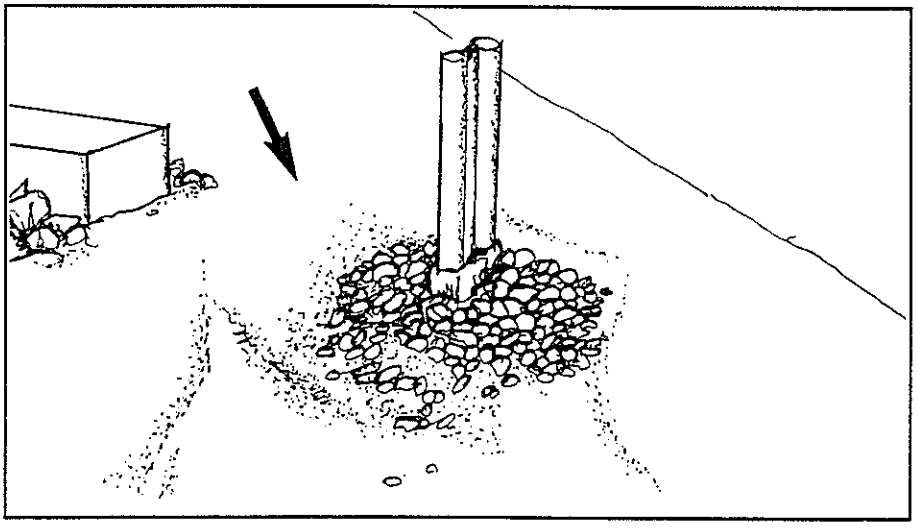

(Drawings copied from photographs)

Figure 2.28 Run 25
Slab piers T2 (second pier out of frame); $\alpha = 30°$;
flow ←; $D_{50} = 15$ mm;
$U_{o,max} = 0.48$ m/s

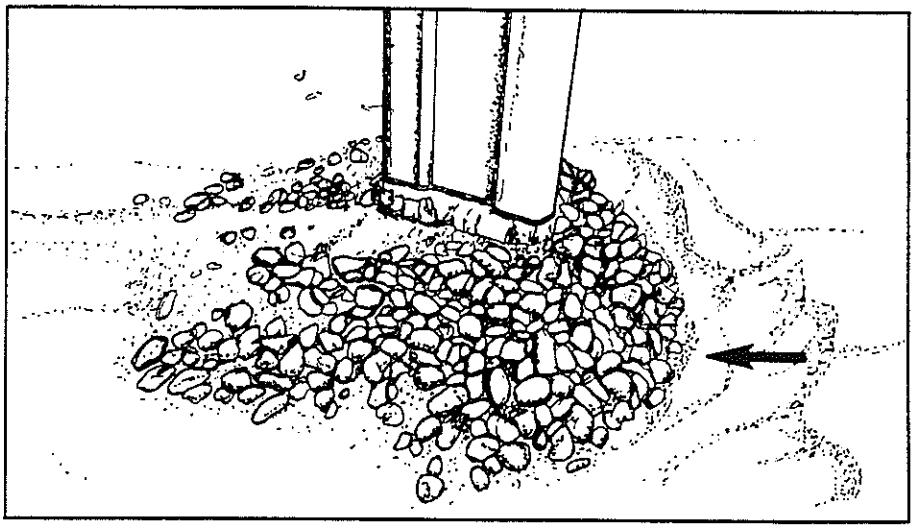

Figure 2.29 Run 26
Slab piers T2; $\alpha = 30°$;
flow →; $D_{50} = 8$ mm;
$U_{o,max} = 0.41$ m/s

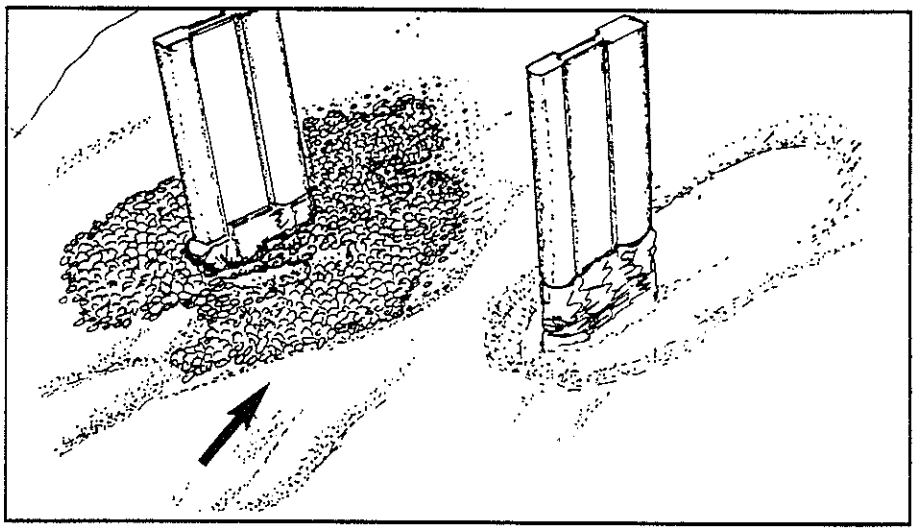

Figure 2.30 Run 27
Slab piers T2; $\alpha = 30°$;
flow →; $D_{50} = 8$ mm;
$U_{o,max} = 0.41$ m/s

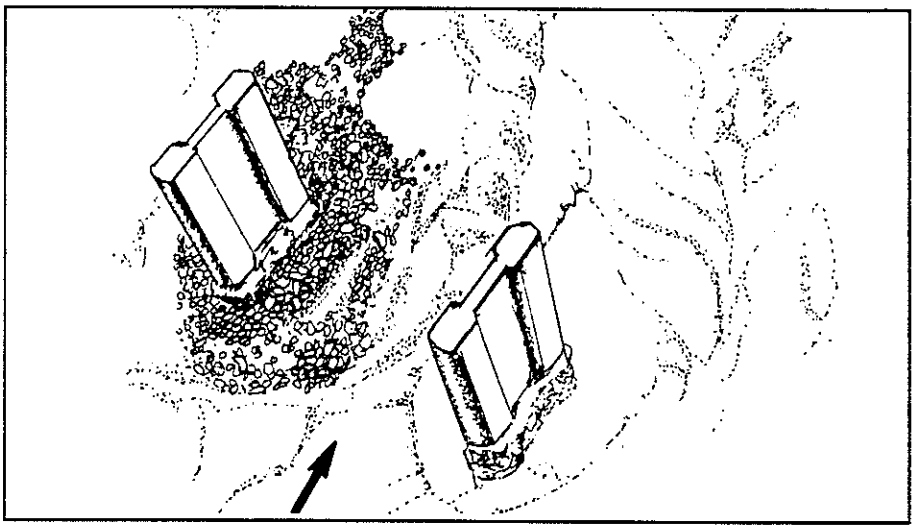

Figure 2.31 Run 28
Slab piers T2; $\alpha = 30°$;
flow →; $D_{50} = 15$ mm;
$U_{o,max} = 0.48$ m/s

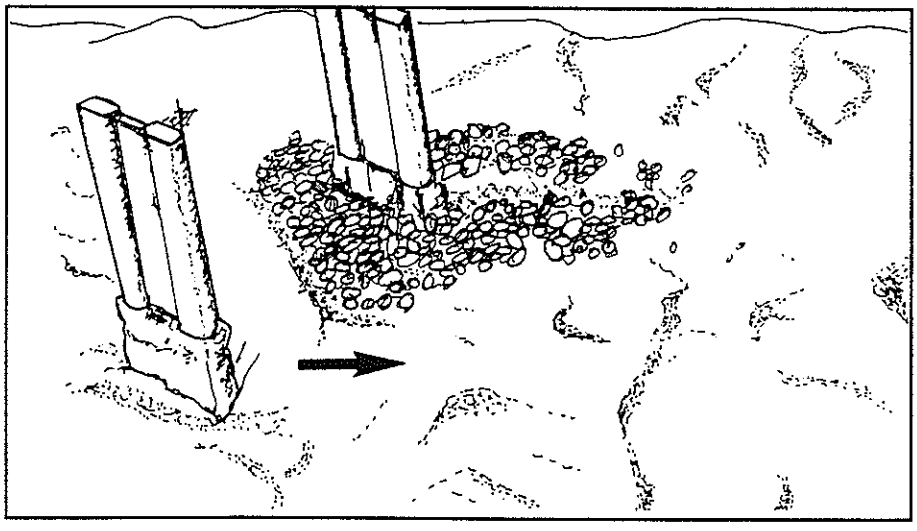

(Drawings copied from photographs)

Figure 2.32 Run 29
Slab pier T2 + abutment:
$\alpha = 30°$; flow →:
(significant proportion of riprap lost adjacent to pier): $D_{50} = 8$ mm.
$U_{o.max} = 0.41$ m/s

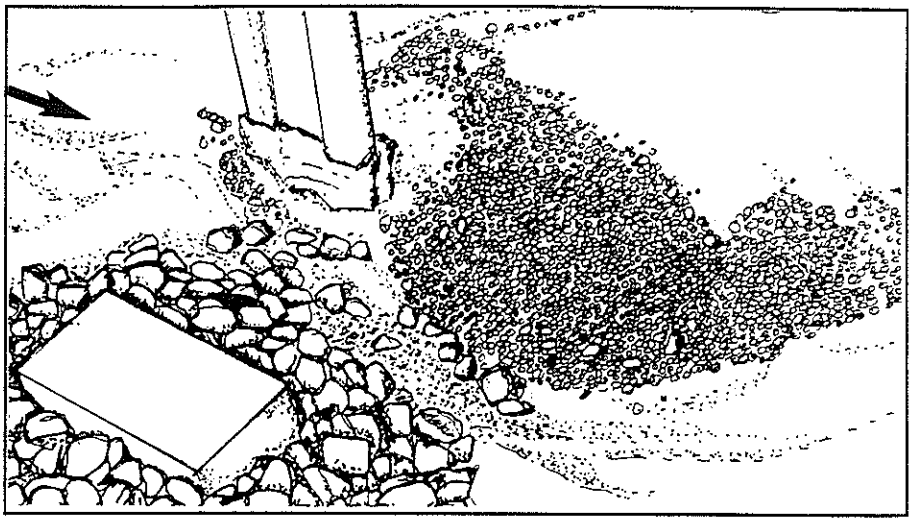

Figure 2.33 Run 30
Slab pier T2 + abutment:
$\alpha = 30°$; flow →:
$D_{50} = 8$ mm:
$U_{o.max} = 0.41$ m/s

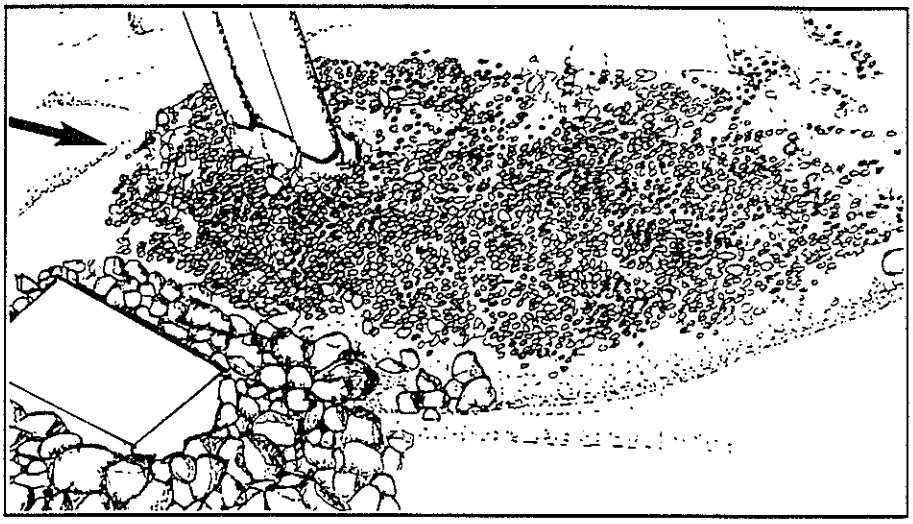

Figure 2.34 Run 31
Slab pier T2 + abutment.
$\alpha = 30°$; flow →:
$D_{50} = 15$ mm:
$U_{o.max} = 0.41$ m/s

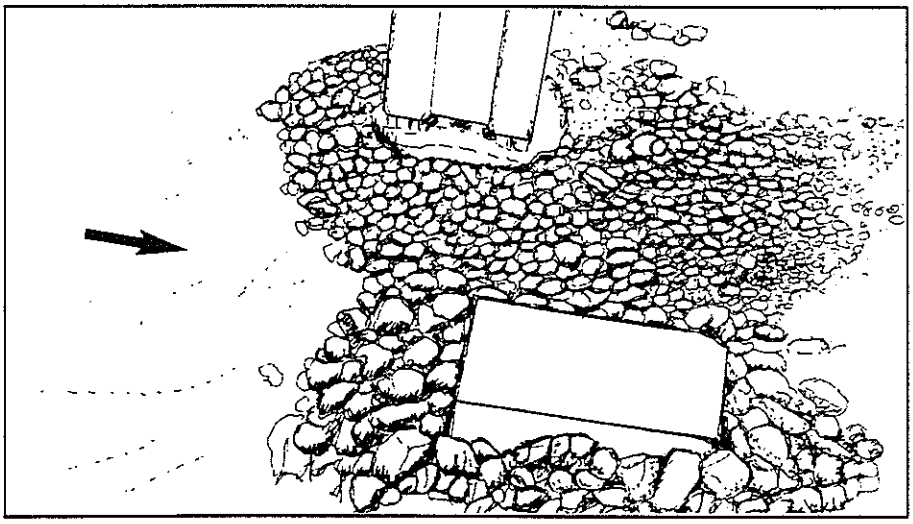

Figure 2.35 Run 32
Slab pier T2 + abutment:
$\alpha = 30°$; flow →:
$D_{50} = 15$ mm:
$U_{o.max} = 0.41$ m/s

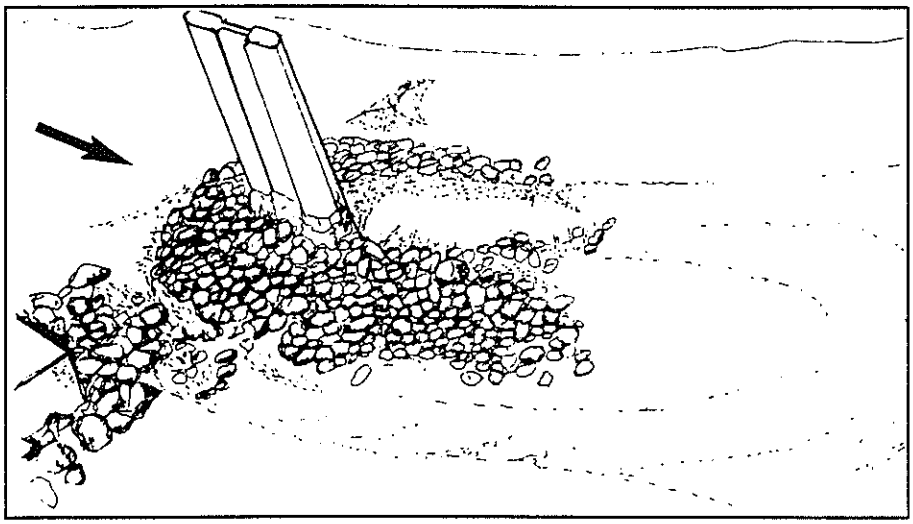

(Drawings copied from photographs)

3. THEORY

3.1 General

The theoretical basis for designing a stable riprap mat around a bridge pier is outlined in Section 3.2 of this report. Where applicable, the theory is compared with relevant experimental data.

3.2 Critical Velocity

The critical velocity is based on the Shields criterion for the entrainment of particles at a large grain Reynolds number:

$$\frac{u_*^2}{g\Delta D} = 0.055 \tag{10}$$

in which D is the particle size,

u_{*c} = $\sqrt{(\tau/\rho)}$ = critical shear velocity,
τ = bed shear stress,
ρ = density of water,
g = gravitational acceleration, and
Δ = submerged relative density of the stones.

It is assumed that $u_{*c}D/\nu > 200$, where ν is the kinematic viscosity of water. This assumption will always apply in any practical design, even at the model scale implied in the present experimental study.

The shear velocity in the approach flow can be related to the mean flow critical velocity U_{0c} by:

$$\frac{U_{0c}}{u_{*c}} = \frac{C}{\sqrt{g}} \tag{11}$$

in which C is the Chézy roughness coefficient given by a Colebrooke-White law adapted for open channel flow (Jansen et al. 1979), which is calculated from:

$$C = 5.75\sqrt{g}\log\left(12\frac{h}{k_s}\right) \tag{12}$$

where h is water depth and k_s is the roughness height. Because Equation 12 is transcendental, it is useful to determine an equivalent algebraic expression. Using a 1/6-power law, an alternative expression for the Chézy coefficient is:

$$C = 6.9\sqrt{g}\left(\frac{h}{k_s}\right)^{1/6} \tag{13}$$

The coefficient of Equation 13 is weakly dependent on h/k_s but has been optimally determined for $1.25 < h/k_s < 2.5$ which is considered appropriate for most practical

applications. For $h/k_s > 2.5$ the result will be slightly conservative (i.e. the velocity U_{0c} will be slightly over-estimated).

Like Neill (1973) we will assume that $k_s = 4D$. Combining Equations 10, 11 and 12 gives:

$$\frac{U_{0c}}{\sqrt{\Delta g D}} = 1.34 \log\left(3\frac{h}{D}\right) \tag{14}$$

Alternatively, using Equation 13 for the Chézy roughness coefficient gives:

$$\frac{U_{0c}}{\sqrt{\Delta g D}} = 1.45\left(\frac{h}{D}\right)^{1/6} \tag{15}$$

The critical velocity at the pier is related to the upstream approach velocity by an acceleration factor A, so that:

$$U_0 = A.U_{0c} \tag{16}$$

Then Equations 14 and 15 become:

$$\frac{U_0}{A\sqrt{\Delta g D}} = 1.34 \log\left(3\frac{h}{D}\right) \tag{17}$$

and

$$\frac{U_0}{A\sqrt{\Delta g D}} = 1.45\left(\frac{h}{D}\right)^{1/6} \tag{18}$$

respectively. For practical purposes these expressions are the same. The acceleration factor A is the ratio U_0/U_{0c} in Table 2.2. Based on the the data in Table 2.2, and data from Hancu (1971), Ramette and Nicollet (1971) and Carstens (1966), the acceleration factors given in Table 3.1 are appropriate:

Table 3.1 Acceleration factors (A) for bridge piers.

Shape	A
Circular and slab piers	0.45
Rectangular and sharp edged piers	0.35

Chiew (1996) proposes that the initiation of scour for a circular pier occurs for $U_0/U_{0c} = 0.3$ which is a lower ratio than that determined in other studies, including the study for this report. The method of estimating the threshold used in this study was the same as that applied by Chiew (i.e. measuring of the depth of scour and extrapolating the result back to $d_s = 0$ to find the applicable U_0 / U_{0c} ratio). Similarly to Chiew, the depth of scour was measured at the deepest point of the scour hole and not just at the nose of the pier. However, the acceleration factor determined by Chiew is low compared to other studies and recommendations, as well as that determined from this study. Consequently, the values given in Table 3.1 will continue to be used in the analysis in this Section 3.

Equation 18 is presented in Figure 3.1 (solid line) with the data from the present study together with the data from Croad (1990) (summarised in Section 2 of this report). Data from Hickman (1989) is also used to fill in the area h/D < 5.0 (very shallow flow). The data from Hickman relate to flow over a groyne or rock fill for which A = 1.0 is appropriate.

With the exception of only a few data points, for $h/D_{50} > 5$, Equation 18 forms a lower (conservative) bound to the data, and all points identified as "failed" lie above this line.

An empirical adjustment can be made to Equation 18 to better fit the trend of the Hickman (1989) data for very shallow flows, namely:

$$\frac{U_0}{A\sqrt{\Delta g D}} = 1.35\left(\frac{h}{D}\right)^{1/6} \qquad (19)$$

The resultant relationships are shown in Figure 3.1 as a dashed line.

Figure 3.2 shows Equations 18 and 19 plotted against the data by Hjorth (1975) and Parola (1993). There were insufficient raw data in the paper by Chiew (1996) to allow his results to be plotted here. Again, Equations 18 and 19 form a lower bound to the data and there is a similar spread in the experimental results which is considered to be quite typical of this type of experiment.

3.3 Embedment

The stability of armour layers overlying a smaller diameter sediment has been studied by Raudkivi and Ettema (1982). According to these authors, the entrainment conditions for a single exposed particle of diameter D overlying a sediment of diameter d can be expressed as a function of the respective shear velocities u_{*D} and u_{*d} as shown in Figure 3.3.

The four zones identified in Figure 3.3 define the following entrainment conditions:

Zone 1 No erosion.

Zone 2 Overpassing:
- if D/d > 0 then the exposed particle moves with a rolling or sliding motion;
- if D/d < 1.0 then the armour particle moves with a bouncing or saltation motion.

Zone 3 Armouring:
- the exposed particle will embed into the underlying sediment providing shelter to particles which are in the wake of the exposed particle.

Zone 4 Erosion:
- all particles on the bed are entrained.

Figure 3.1 $U_0 (\Delta g D_{50})^{-1/2}$ as a function of h/D_{50} based on the results from the present study, as well as data from Hickman (1989) and Croad (1990).

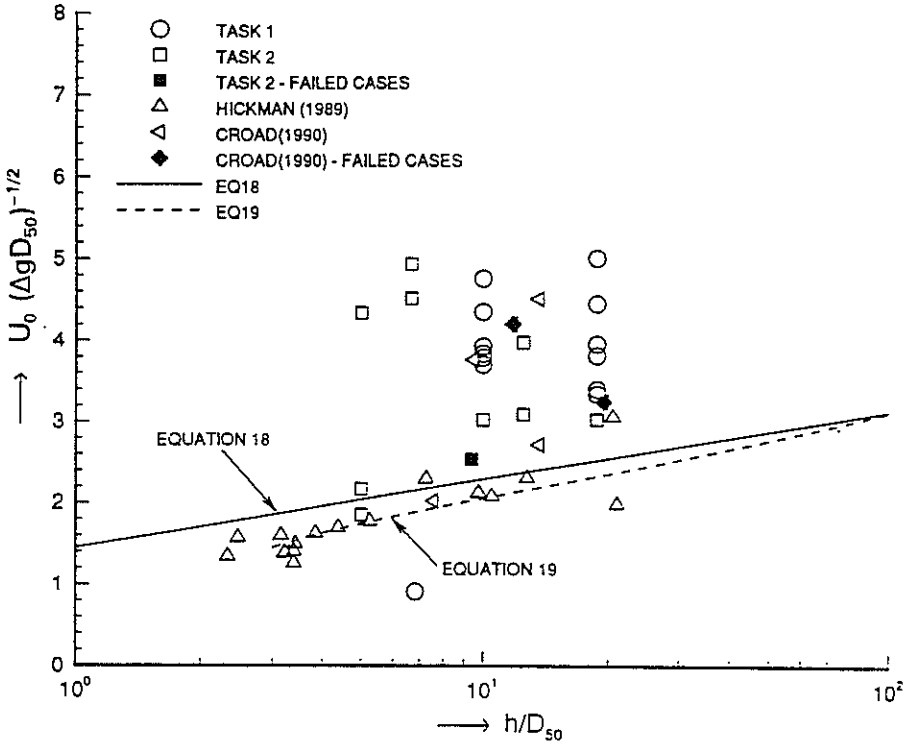

Figure 3.2 $U_0 (\Delta g D_{50})^{-1/2}$ as a function of h/D_{50} based on data from Hjorth (1975) and Parola (1993).

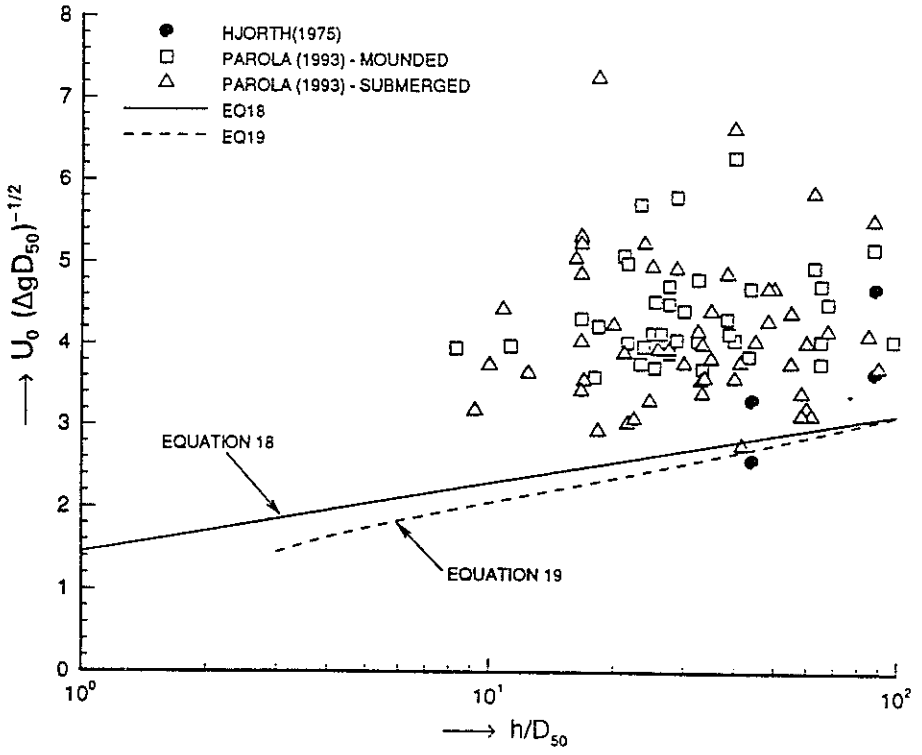

Figure 3.3 Entrainment conditions for a single particle of diameter D on a bed sediment of diameter d (after Raudkivi and Ettema 1982).

The following nomenclature is used for Zones 1 to 4:

Zone 1: No erosion.

Zone 2: Overpassing:
if D/d > 0 then the exposed particle moves with a rolling or sliding motion:
if D/d < 1.0 then the armour particle moves with a bouncing or saltation motion.

Zone 3: Armouring: the exposed particle will embed into the underlying sediment providing shelter to particles which are in the wake of the exposed particle.

Zone 4: Erosion - all particles on the bed are entrained.

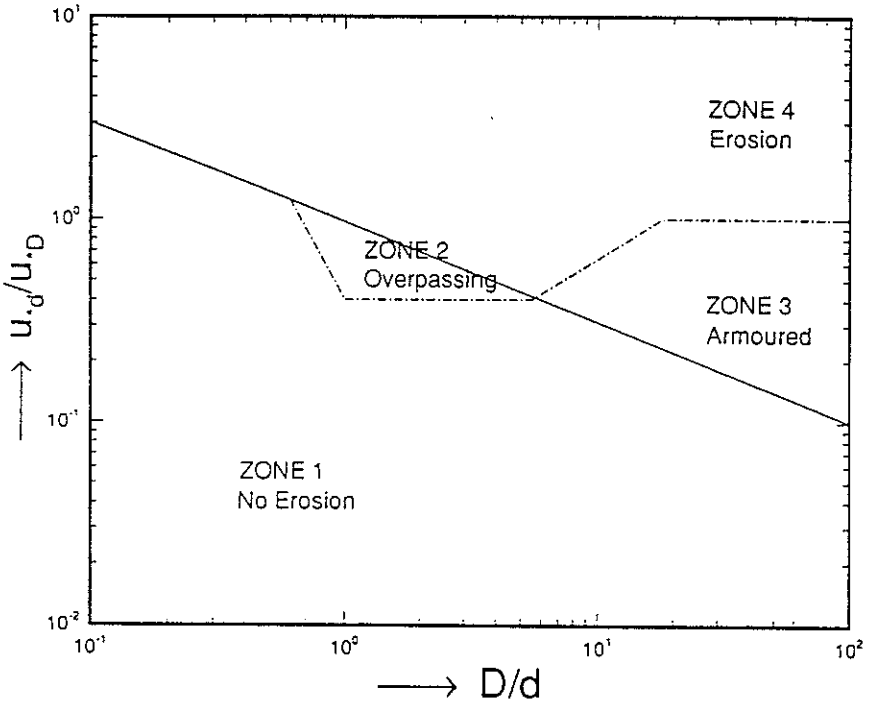

For $u_{*d}/u_{*D} < 1.0$ then embedment of the exposed particle into the underlying sediment is achieved if D/d > 17. If $u_{*d}/u_{*D} < 0.5$, then this condition is achieved for D/d > 10. Whittaker et al. (1989) found that D/d > 10 was a satisfactory condition for the design of placing large stones in a river bed as a stabilisation technique.

In the present study, the embedment criterion was met for the fine 0.29-mm diameter bed sediment. Inspection of Figures 2.4–2.35 shows that the riprap mat held together better for this size of sediment and the riprap stones tended to be less exposed to the flow compared to the experiments using the 2.2-mm bed sediment. Similarly, this is confirmed from Croad (1990), from the experiences with block ramps (Whittaker and Jäggi 1986), and from river stabilisation methods using placed blocks (Whittaker et al. 1989).

3.4 Filter Layer

Specifications to determine the required grading curve for a filter layer between the riprap and the bed sediment are given in Section 1.2 of this report. The specification given by Equation 4 was achieved in the present study and can be recommended for general use.

Inspection of Figures 2.4 – 2.35 shows that burying of the riprap adjacent to a pier was avoided when a filter layer was used. Because the filter and embedment requirements lead to incompatible grading requirements, the filter layer must be limited to the leading half of the riprap mat and adjacent to the pier and around the piles. This then leaves the downstream end and sides of the riprap mat to embed into the sediments as the bed levels degrade.

4. DISCUSSION

4.1 General

Previously used formulae for determining the size of riprap to put around bridge piers can be compared with Equations 18 or 19. The expression by Breusers et al. (1977) can be reduced to:

$$\frac{U_0}{A\sqrt{\Delta g D_{50}}} = 1.2 \tag{20}$$

which is the original expression by Isbash (1935) when A = 1.0. The expression by Maynord (1978) can be rearranged to:

$$\frac{U_0}{A\sqrt{\Delta g D_{50}}} = 1.29\left(\frac{h}{D_{50}}\right)^{1/6} \tag{21}$$

in which A = 1/1.25 is suggested for circular piers (see Table 1.1). The expression by Croad (1990), when modified to a suitable algebraic form, becomes approximately:

$$\frac{U_0}{A\sqrt{\Delta g D_{50}}} = 2.0\left(\frac{h}{D_{50}}\right)^{1/6} \tag{22}$$

in which A = 1/1.20. When compared against Equation 18, Equation 21 will give very conservative results for most practical problems. Equation 22 is very similar to Equation 15 and, using the value of A = 1/1.25, will give slightly smaller riprap sizes than determined from Equations 18 or 19 and Table 3.1. The earlier expression by Croad (1990) will tend to give non-conservative results as already identified in Section 1 of this report.

The expression by Parola (1993) for circular piers (Equation 7) is almost identical to that by Breusers et al. (1977) given in Equation 20 based on A = 1.0. According to Parola, the coefficient on the right hand side of Equation 21 should be in the range 0.8 to 1.2 depending on the ratio of the pier to size of riprap. Obviously the expressions by Parola (1993) lead to much higher critical velocities for a given riprap size compared to the results of this present study.

The expression by Chiew (1996) can be rearranged to the dimensionless form:

$$\frac{U_0}{A\sqrt{\Delta g D_{50}}} = 1.8 \left(\frac{h}{D_{50}} \right)^{1/6} \tag{23}$$

in which A = 0.3 for circular piers. This expression is very similar to Equation 18. If A = 0.45 is accepted for circular piers, as proposed by the writer, then the coefficient on the right hand side of Equation 23 becomes 1.2 which is even closer to the coefficient in Equation 18.

Figures 3.1 and 3.2 show that Equations 18 and 19 give reasonable but conservative estimates for the required riprap median size over a wide range of h/D_{50} values. This equation has been derived completely independently of the data. In practice, critical velocities up to twice those predicted can be tolerated for many conditions. The ability of the flow to entrain stones is not the only control on the overall stability of the riprap mat.

Equation 19 forms a lower bound to cases in which failure was observed. It also fits the Hickman (1989) data reasonably well. This expression is therefore recommended as the basis for the design of riprap scour-protection mats around bridge piers along with the other requirements outlined in the Appendix to this report. Riprap protection mats so designed can operate under conditions involving large deformations of the river bed. A complete design procedure is specified in the Appendix.

Because the riprap generally is required to protect the pier against relatively low probability events and, since Equation 19 forms a lower bound to the data, a low factor of safety of 1.25 is recommended.

4.2 Design Procedure

A design procedure is outlined in the Appendix. The design procedure incorporates the findings of this study. However, the following additional features or constraints are highlighted:

1. The riprap layer should be placed below the trough of any dunes that may form in the river during floods. The formula by van Rijn (1982) is recommended to calculate the amplitude of such dunes. This formula has been extensively tested and is considered by the writer to give reasonable results based on experience from physical models of the Hutt River (Ewen Floodway) and Manawatu River (Fitzroy Bend).

2. The spacing between the piers has not been tested as a variable. However, the results are based on a pier spacing in the order of 16 m measured centre to centre and at skew angles up to 30°. The pier spacing is reasonably representative of slab bridges built in the 1940-70 era. For very short spacings (say less than 13 m) and very high skew angles (greater than 30°), specific model tests will be warranted.

3. For a pier with abutments, the design should be based on a velocity taken at a midpoint between the abutment and the pier (rather than on the upstream approach velocity which will be lower). A procedure is suggested in the Appendix for calculating this velocity. However, for very complicated geometries or very high skew angles, a physical model will be warranted in which case the riprap can be tested directly.

5. REFERENCES

Breusers, H.N.C., Nicollet, G., Shen, H.W. 1977. Local scour around cylindrical piers. *Journal of Hydraulic Research 15(3):* 211-252.

Carstens, M.R. 1966. Similarity laws for localized scour. *Journal of the Hydraulics Division, ASCE (American Society of Civil Engineers), 92(HY3):* 13-36.

Chiew, Y.M. 1996. Mechanics of riprap failure at bridge piers. *Journal of Hydraulic Engineering, ASCE, 121(9):* 635-643.

Croad R.N. 1990. Effect of riprap on pier scour. *Central Laboratories Report No. 90-23201*, Works Consultancy Services, Lower Hutt, New Zealand.

Engels, H. 1929. Experiments pertaining to the protection of bridge piers against undermining. *Hydraulic Laboratory Practice*, J.R. Freeman (Ed.), American Society of Mechanical Engineers, New York, N.Y.

Farraday, R.V., Charlton, F.G. 1983. *Hydraulic factors in bridge design.* Hydraulics Research Ltd, Wallingford. Produced by Thomas Telford Ltd, U.K.

Gales, R.R. 1938. The principles of river-training for railway bridges, and their application to the case of the Harding Bridge over the Lower Ganges at Sara. *Journal of the Institution of Civil Engineers (UK) 10(2):* 136-224.

Hancu, S. 1971. Sur le calcul des affouillements locaux dans la zone du pont. *Proceedings, 14th IAHR Congress*, Paris, 3: 299-313.

Hickman, W.E. 1989. Design of riprap in groynes under overtopping flow conditions. *Central Laboratories Report No. 89-23111*, Works Consultancy Services, Lower Hutt.

Hjorth, P. 1975. Studies on the nature of local scour. *Bulletin Series A No. 46*, Department of Water Resources Engineering, Lund Institute of Technology, University of Lund, Sweden.

Isbash, S.V. 1935. Construction of dams and other structures by dumping stones into flowing water. *Transactions of the Research Institute of Hydrotechnology, Leningrad, 17*: 12-66.

Jansen, P.Ph., van Bendegom, L., van den Berg, L., de Vries, M., Zanen, A. 1979. *Principles of river engineering. The nontidal alluvial river*. Pitman, London.

Maynord, S.T. 1978. *Practical rip rap design.* Waterways Experiment Station, U.S. Army Engineers, Vicksburg, USA.

Melville, B.W. 1975. Local scour at bridge sites. *University of Auckland School of Engineering Report No. 117*, School of Engineering, University of Auckland.

Melville, B.W., Sutherland, A.J. 1987. Design method for local scour at bridge piers. *Journal of Hydraulic Engineering, ASCE, 14(10):* 1210-1293.

Neill, C.R. (Ed.) 1973. *Guide to bridge hydraulics.* Roads and Transportation Association, University of Toronto Press, Canada.

Parola, A.C. 1993. Stability of riprap at bridge piers. *Journal of Hydraulic Engineering, ASCE, 119(10):* 1080-1093.

Posey, C.J. 1974. Tests of scour protection for bridge piers. *Journal of the Hydraulic Division, ASCE, 100(HY12):* 1773-1783.

Ramette, M., Nicollet, G. 1971. Affouillements au voisinage des piles de ponts cylindriques ou circulaires. *Proceedings, 14th IAHR Congress, Paris, 3*: 315-322.

Raudkivi, A.J., Ettema, R. 1982. Stability of armour layers in rivers. *Journal of the Hydraulics Division, ASCE, 108(HY9):* 1047-1057.

Simons, D.B., Senturk, F. 1977. *Sediment transport technology.* Water Resources Publications, Fort Collins, Colorado, USA.

Sutherland, A.J. (Ed.) 1986. *Reports on bridge failures.* Road Research Unit Occasional Paper, National Roads Board, Wellington, New Zealand.

van Rijn, L.C. 1982. The prediction of bed-forms and alluvial roughness. *Proceedings from Euromech 156, Mechanics of Sediment Transport*, Technical Faculty of Istanbul, Turkey, July 12-14, 1982.

Whittaker, J.G., Jäggi, M. 1986. Blockschwellen. *Mitteilungen Nr. 91*, Versuchsanstalt für Wasserbau, Hydrologie und Glaziologie, Zürich.

Whittaker, J.G., Hickman, W.E., Croad, R.N. 1989. Riverbed stabilisation with placed blocks. *Transactions of the Institution of Professional Engineers, New Zealand, 16(2/CE):* 82-90.

APPENDIX. PROCEDURE FOR THE DESIGN OF RIPRAP MATS AROUND BRIDGE PIERS FOR SCOUR PROTECTION

PROCEDURE FOR THE DESIGN OF RIPRAP MATS AROUND BRIDGE PIERS FOR SCOUR PROTECTION

PROCEDURE

1. Input parameters are:
   - Water depth h and upstream approach velocity U_0.
     The depth should take into account any local or general scour at the site.
   - Bed sediment median size d_{50} and geometric standard deviation $\sigma_g = d_{85}/d_{50}$.
   - Pier width B, length L, shape and angle of attack of the flow α in degrees.

     As a minimum, an angle of $\alpha = 20°$ should be adopted.

- Note that the velocity U_0 must be the depth-averaged velocity in the vicinity of the pier, and not the average velocity for the whole of the river cross-section.

- Thus, if the discharge is Q, the wetted cross-sectional area is A_0 and and the hydraulic depth (area divided by the surface with of the river) is h_0 , the correct velocity to take will be approximately:

$$U_0 = \frac{Q}{A_0}\left(\frac{h}{h_0}\right)^{2/3} \qquad \text{(A1)}$$

- If the bridge alignment is skewed, the Equation A1 should be modified to:

$$U_0 = \frac{Q}{A_0 \sin \alpha}\left(\frac{h}{h_0}\right)^{2/3} \qquad \text{(A2)}$$

- For mid-river piers where the bridge also has projecting abutments, the approach velocity U_0 is the velocity that exists after allowing for the contraction of the flow between the abutments. The velocity must be based on the area between the abutments projected onto a plane at right angles to the flow lines (as per Equation A2).

- For a pier adjacent to an abutment which projects into the flow, the appropriate velocity to take for U_0 is the velocity at a mid point between the abutment and the pier. The velocity can be calculated using a depth-averaged turbulent flow mathematical model which will take into account the contraction and acceleration of the flow past the abutment.

- Proprietary turbulence modelling systems such as FIDAP or PHOENIX are suitable but require specialised experience to operate. Both systems will represent the separation of the flow around the abutment, although the three-dimensional velocity field immediately adjacent to the abutment will only be approximately correct.

- For very complex geometries, or very high abutment skew angles, a physical model will be warranted, in which case the riprap system can be tested directly.

---

2. Compute the effective pier width $B_e = K_\alpha B$ in which
   K_α is 1.2 for square piers and
   K_α equals 1.0 for circular piers.

   For slab piers calculate B_e from:

$$B_e = B \cos \alpha + L \sin \alpha \tag{A3}$$

   in which α is the angle of attack of the flow relative to the transverse axis of the bridge pier.

---

3. Compute the particle parameter D_* (a dimensionless number) and critical shear velocity u_{*c} for the bed material from:

$$D_* = d_{50} \left(g\Delta/\nu^2\right)^{1/3} \tag{A4}$$

$$u_{*c} = \sqrt{\Delta \; g \; d_{50} \; \theta_c} \tag{A5}$$

   in which ν is the kinematic viscosity of water,
   g is the gravitational acceleration,
   Δ is the submerged relative density of the sediment and
   θ_c is the Shields parameter which can be computed from:

$$\begin{aligned}
D_* &\le 4 && \theta_c = 0.24 \; D_*^{-1} \\
4 < D_* &\le 10 && \theta_c = 0.14 \; D_*^{-0.64} \\
10 < D_* &\le 20 && \theta_c = 0.04 \; D_*^{-0.10} \\
20 < D_* &\le 150 && \theta_c = 0.013 \; D_*^{0.29} \\
150 < D_* & && \theta_c = 0.055
\end{aligned} \tag{A6}$$

---

4. Compute the bed friction roughness coefficient C and bed friction shear velocity u_* from:

$$C = 5.75\sqrt{g} \log\left(\frac{4h}{D_{85}}\right) \tag{A7}$$

$$u_* = U_0 \frac{\sqrt{g}}{C} \tag{A8}$$

---

5. Compute the transport stage parameter:

$$T = \frac{u_*^2 - u_{*o}^2}{u_{*o}^2} \tag{A9}$$

---

6. Compute the bed-form (dune) height Λ and minimum depth below the bed $\delta = \frac{1}{2}\Lambda$ of the surface of the riprap. This ensures that the riprap will be at or below the trough level of the bed-forms. However, a minimum value of $\delta = 1.0$ m is recommended.

   The bed-form height can be determined from the formula by van Rijn (1982), namely:

$$\frac{\Lambda}{h} = 0.11\left(\frac{d_{50}}{h}\right)^{0.3}(1 - e^{-0.5T})(25 - T) \tag{A10}$$

---

7. Compute the acceleration factor A from Table A1.

Table A1. Acceleration factors (A) for piers.

Shape	A
Circular and slab piers	0.45
Square and sharp edged piers	0.35

---

8. Compute the required riprap median size D_{50} as the larger of the two values from the entrainment and embedment requirements

$$\frac{U_0}{A\sqrt{\Delta g D_{50}}} = \frac{1.35}{F}\left(\frac{h}{D_{50}}\right)^{1/6} \tag{A11}$$

$$D_{50} = 17\ d_{50} \tag{A12}$$

   in which F is the factor of safety adopted for the design.

---

9. Determine the filter requirements from:

$$\frac{d_{50}\ (\text{layer}\ 1)}{d_{50}\ (\text{layer}\ 2)} < 25$$

$$4 < \frac{d_{15}\ (\text{layer}\ 1)}{d_{15}\ (\text{layer}\ 2)} < 20 \qquad \text{(A13)}$$

$$\frac{d_{15}\ (\text{layer}\ 1)}{d_{85}\ (\text{layer}\ 2)} < 5$$

The thickness of the filter layer should be equal to the median size of the riprap. The placement of the filter material should be as indicated in Figure 2.3 in Section 2 of main report.

---

10. The grading for the riprap material should be determined from $D_{max}/D_{50} \leq 2.0$ and $D_{50}/D_{15} \leq 2.0$.

---

11. The minimum thickness of the riprap layer is determined from $t = 2D_{50}$.

---

12. The riprap mat should extend at least a distance $2B_e$ either side and a distance $1.5B_e$ to the front of the pier and a distance $3B_e$ to the downstream side of the pier. The general shape of the riprap around the pier should be as indicated in Figure 2.3 in Section 2 of main report.

Figure 2.3 Plan layout of the riprap and filter layers around two types of pier.
(a) Square pier

B = pier size

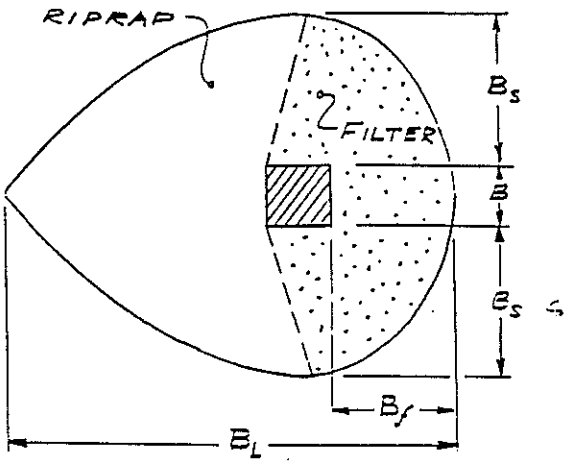

(b) Slab pier

B_e = effective width of slab pier

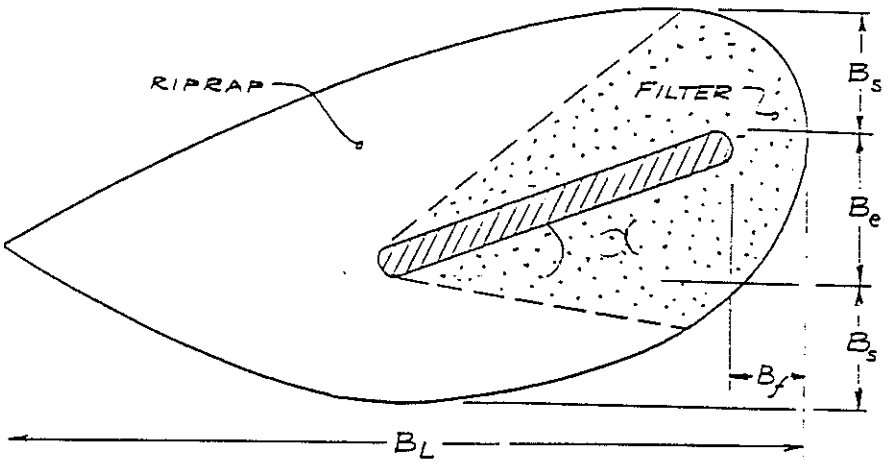

(c) Representative cross-section view of a slab pier.

t = thickness of riprap mat

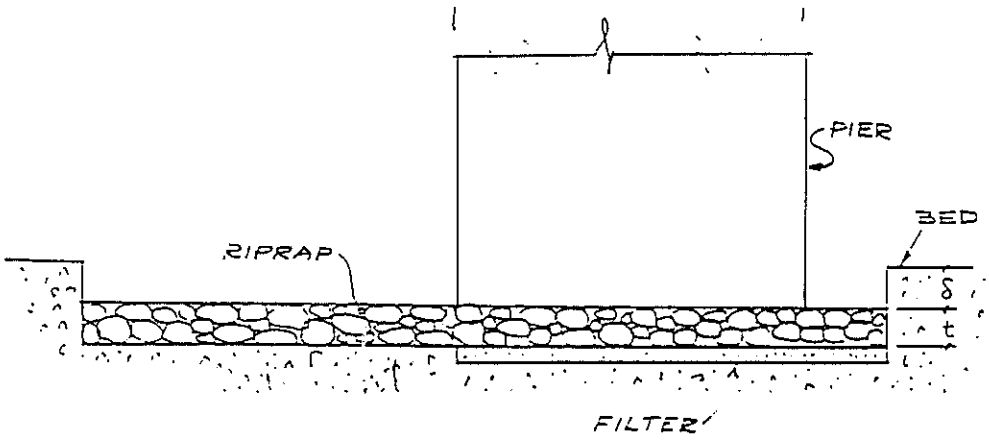

(from Section 2 of this report, see S2.9 for explanation of other symbols)

DESIGN FOR RIPRAP MAT FOR A CIRCULAR BRIDGE PIER: Example

Problem

To design a riprap mat for a 2.4 m circular pier,
assuming a factor of safety of F = 1.25,
for the following conditions:
$U_0 = 3.0$ m/s, $h = 6.0$ m, $d_{50} = 20$ mm, $\sigma_g = 2.5$ and $\Delta = 1.65$.
The acceleration due to gravity is 9.8 m/s^2.

Calculations

$$d_{85} = \sigma_g \, d_{50} = 0.05 \text{ m}$$

$$C = 5.75 \sqrt{g} \log \left(12 \frac{h}{3 d_{85}} \right) = 48.3 \text{ m}^{1/2}/\text{s}$$

$$D_* = d_{50} \left(\frac{\Delta g}{\nu^2} \right)^{1/3} = 475$$

$$\theta_c = 0.055$$

$$u_* = U_0 \frac{\sqrt{g}}{C} = 0.19 \text{ m/s}$$

$$T = \frac{u_*^2 - u_{*c}^2}{u_{*c}^2} = 1.1$$

$$\Lambda = 0.11 h \left(\frac{d_{50}}{h} \right)^{0.3} \left(1 - e^{-0.5T}\right) (25 - T) = 1.22 \text{ m}$$

$$\delta = \frac{1}{2} \Lambda = 0.6 \text{ m}$$

From Equation A11 the required riprap size is:

$$D_{50} = 1.46 \text{ m}$$

From Equation A12 it is verified that $D_{50} > 17 d_{50}$.

Conclusion

The riprap mat required has median size D_{50} = 1.46 m, and it should be at least 2.9 m thick, and extend 4.8 m either side, 3.6 m in front, and 7.2 m downstream of the pier.

The filter layer under the riprap mat should be 1.46 m thick with
median size = 58 mm < d_{50} (filter) < 500.

A value of d_{50} (filter) = 100 mm conforms reasonably well with the other requirements of Equation A13.